

AD-A038 759

NAVAL POSTGRADUATE SCHOOL MONTEREY CALIF  
THE FINITE ELEMENT METHOD APPLIED TO FLOWS IN TURBOMACHINES.(U)  
DEC 76 V F GAVITO

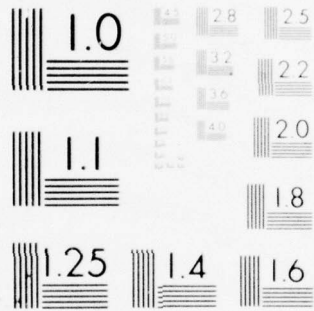
F/G 20/4

UNCLASSIFIED

NL

1 of 2  
AD A038759





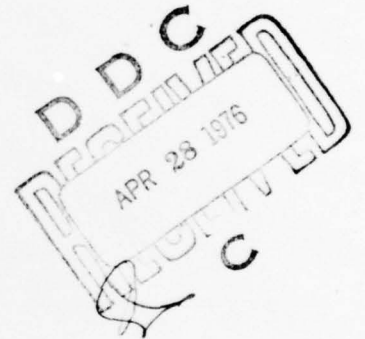
MICROCOPY RESOLUTION TEST CHART  
NATIONAL BUREAU OF STANDARDS (1963)

ADA 038759

P

# NAVAL POSTGRADUATE SCHOOL

Monterey, California



## THESIS

THE FINITE ELEMENT METHOD APPLIED TO FLOWS IN  
TURBOMACHINES

by

Valentin Francisco Gavito, Jr.

December 1976

Thesis Advisor:

D.J. Collins

Approved for public release; distribution unlimited.

AD NO. \_\_\_\_\_  
DDC FILE COPY.

REPORT DOCUMENTATION PAGE		READ INSTRUCTIONS BEFORE COMPLETING FORM
1. REPORT NUMBER	2. GOVT ACCESSION NO.	3. RECIPIENT'S CATALOG NUMBER
4. TITLE (and Subtitle)		5. TYPE OF REPORT & PERIOD COVERED
6 The Finite Element Method Applied To Flows In Turbomachines		7 Master's Thesis, December 1976
7. AUTHOR(s)		8. CONTRACT OR GRANT NUMBER(s)
10 Valentin Francisco Gavito, Jr		
9. PERFORMING ORGANIZATION NAME AND ADDRESS		10. PROGRAM ELEMENT, PROJECT, TASK AREA & WORK UNIT NUMBERS
Naval Postgraduate School Monterey, California 93940		
11. CONTROLLING OFFICE NAME AND ADDRESS		12. REPORT DATE
Naval Postgraduate School Monterey, California 93940		11 December 1976
14. MONITORING AGENCY NAME & ADDRESS (if different from Controlling Office)		13. NUMBER OF PAGES
		12 125 P.
		18. SECURITY CLASS. (of this report)
		Unclassified
		18a. DECLASSIFICATION/DOWNGRADING SCHEDULE
16. DISTRIBUTION STATEMENT (of this Report)		
Approved for public release; distribution unlimited.		
17. DISTRIBUTION STATEMENT (of the abstract entered in Block 20, if different from Report)		
18. SUPPLEMENTARY NOTES		
19. KEY WORDS (Continue on reverse side if necessary and identify by block number)		
Finite Element Method Turbomachines		
20. ABSTRACT (Continue on reverse side if necessary and identify by block number)		
The finite element method is applied to the two-dimensional, inviscid, compressible radial equilibrium equation for axial compressors. Isoparametric elements are used along with three-point Gaussian integration for stiffness matrix evaluation. The radial equilibrium equation is put into quasi-harmonic form for stream function formulation and results are presented using an isentropic flow assumption. Axial velocity profiles at rotor and stator blade edges are compared with published performance data →		

→ of the NASA Task-1 stage transonic compressor and with numerical finite element results of Hirsch and Warzee.

ADDITIONAL FOR	
NTIS	White Section <input checked="" type="checkbox"/>
DIC	Buff Section <input type="checkbox"/>
UNANNOUNCED	<input type="checkbox"/>
JUSTIFICATION	
BY	
DISTRIBUTION/AVAILABILITY CODES	
Dist.	AVAIL. CODE/SPECIAL
A	

THE FINITE ELEMENT METHOD APPLIED TO FLOWS IN  
TURBOMACHINES

by

Valentin Francisco Gavito, Jr.  
Lieutenant, United States Navy  
B.S.M.E., Southern Methodist University, 1970

Submitted in partial fulfillment of the  
requirements for the degree of

MASTER OF SCIENCE IN AERONAUTICAL ENGINEERING

from the  
NAVAL POSTGRADUATE SCHOOL  
December 1976

Author:

*Valentin Francisco Gavito, Jr.*

Approved by:

*Daniel J. Collins*

Thesis Advisor

*Raymond A. Shoenue*

Second Reader

*Richard W. Bell*

Chairman, Department of Aeronautics

*Albert N. Johnson*

Dean of Science and Engineering

## ABSTRACT

The finite element method is applied to the two-dimensional, inviscid, compressible radial equilibrium equation for axial compressors. Isoparametric elements are used along with three-point Gaussian integration for stiffness matrix evaluation. The radial equilibrium equation is put into quasi-harmonic form for stream function formulation and results are presented using an isentropic flow assumption. Axial velocity profiles at rotor and stator blade edges are compared with published performance data of the NASA Task-1 stage transonic compressor and with numerical finite element results of Hirsch and Warzee.

## TABLE OF CONTENTS

I.	INTRODUCTION.....	7
A.	PROBLEM STATEMENT AND OBJECTIVE.....	7
II.	THEORY.....	10
A.	THE DERIVATION OF THE RADIAL EQUILIBRIUM EQUATION.....	10
B.	THE FINITE ELEMENT METHOD APPLIED TO THE RADIAL EQUILIBRIUM EQUATION.....	20
C.	NUMERICAL INTEGRATION OF THE STIFFNESS MATRIX AND SOLUTION PROCEDURE.....	28
1.	Numerical integration of the stiffness matrix.....	28
2.	Solution procedure.....	32
a.	Discretization.....	32
b.	Initialization.....	32
c.	Calculation of thermodynamic variables.....	34
d.	Calculate matrices.....	37
e.	Solve system of equations.....	37
f.	Perform relaxation iteration.....	37
g.	Update velocity and density profiles.....	37
h.	Test for convergence of $\psi$ .....	38
i.	Summary.....	38
III.	THE PROGRAM.....	40
A.	OVERALL FLOWCHART AND DESCRIPTION.....	40
B.	THE MAIN PROGRAM.....	43
1.	The input routine.....	43
a.	category 1.....	43
b.	category 2.....	43
c.	category 3.....	43
d.	category 4.....	43

e. category 5.....	43
f. category 6.....	44
g. category 7.....	44
h. category 8.....	44
i. category 9.....	44
j. category 10.....	44
k. category 11.....	44
l. category 12.....	44
2. Stiffness matrix evaluation.....	50
3. Solution of system of equations.....	52
4. Iteration schemes.....	52
5. The output routine.....	53
C. THE SUBROUTINES.....	53
1. Subroutine shape.....	54
2. Subroutine jacob.....	54
3. Subroutine sline.....	55
4. Subroutine fcal.....	58
5. Subroutine vel.....	61
6. Subroutine mplot.....	66
IV. TEST CASES AND RESULTS.....	67
V. CONCLUSIONS AND RECOMMENDATIONS FOR FURTHER STUDY.....	70
Appendix A: COMPUTER PROGRAM.....	76
Appendix B: SAMPLE INPUT DATA.....	100
Appendix C: SAMPLE OUTPUT LISTING.....	107
Appendix D: CALCULATION OF ROTOR ELEMENT FLOW ANGLES...	117
LIST OF FIGURES.....	122
LIST OF REFERENCES.....	123
INITIAL DISTRIBUTION LIST.....	125

## I. INTRODUCTION

### A. PROBLEM STATEMENT AND OBJECTIVE

The prediction of meridional flows within turbomachines, be they compressors or turbines, is a difficult but important part of the design process. The difficulty arises from the presence of three-dimensional and viscous effects within all turbomachines and the importance arises from the necessity to design accurately and efficiently.

To simplify the problem of viscous, three-dimensional analysis, Wu [Ref.1] showed that this complicated flow may be analyzed by solving two interrelated flows: one being the blade-to-blade flow describing the flow between rotating blades and the other being the meridional through flow which describes the radial equilibrium. These flows are depicted in Fig 1. In addition, an inviscid and axi symmetric assumption is made in the through-flow thereby simplifying the flow to a two-dimensional, axi symmetric, inviscid, and compressible analysis.

Three methods may be found in current reports regarding the solution of the radial equilibrium equation. The first two are the streamline curvature method [Ref.2,3,and 4] and the matrix method [Ref.5 and 6] which is basically a finite difference technique. The third, a relatively new method, is the finite element method. As shown by Hirsch and Warzee [Ref.7]', the solution of the radial equilibrium equation by the finite element method is achieved by arranging the

equation for the stream function in quasi-harmonic form.

Due to the excellent results reported in Ref.7 and to further the research effort for finite element techniques in fluid flow problems, the purpose of this thesis is two fold. Firstly, the goal was to formulate a computer program for solution of the radial equilibrium equation paralleling the steps as presented by Hirsch and Warzee. Secondly, after suitable verification of computer results with those of Hirsch and Warzee, the goal was to compare computer predicted flows with measured performance data of the Naval Post Graduate School's transonic compressor.

The purpose of this paper is to present a report on the results obtained thus far. In Section II, the derivation of the radial equilibrium equation is presented followed by the application of the finite element method to this equation. Section III describes the computer program in some detail. Section IV contains selected test cases which were used in program testing and checking. In Section V, conclusions are presented along with recommendations for further study and work on the project. The appendices contain the program listing along with a sample test case for reference by the user. In addition, a list of references is contained for further reading on the subject of this paper.

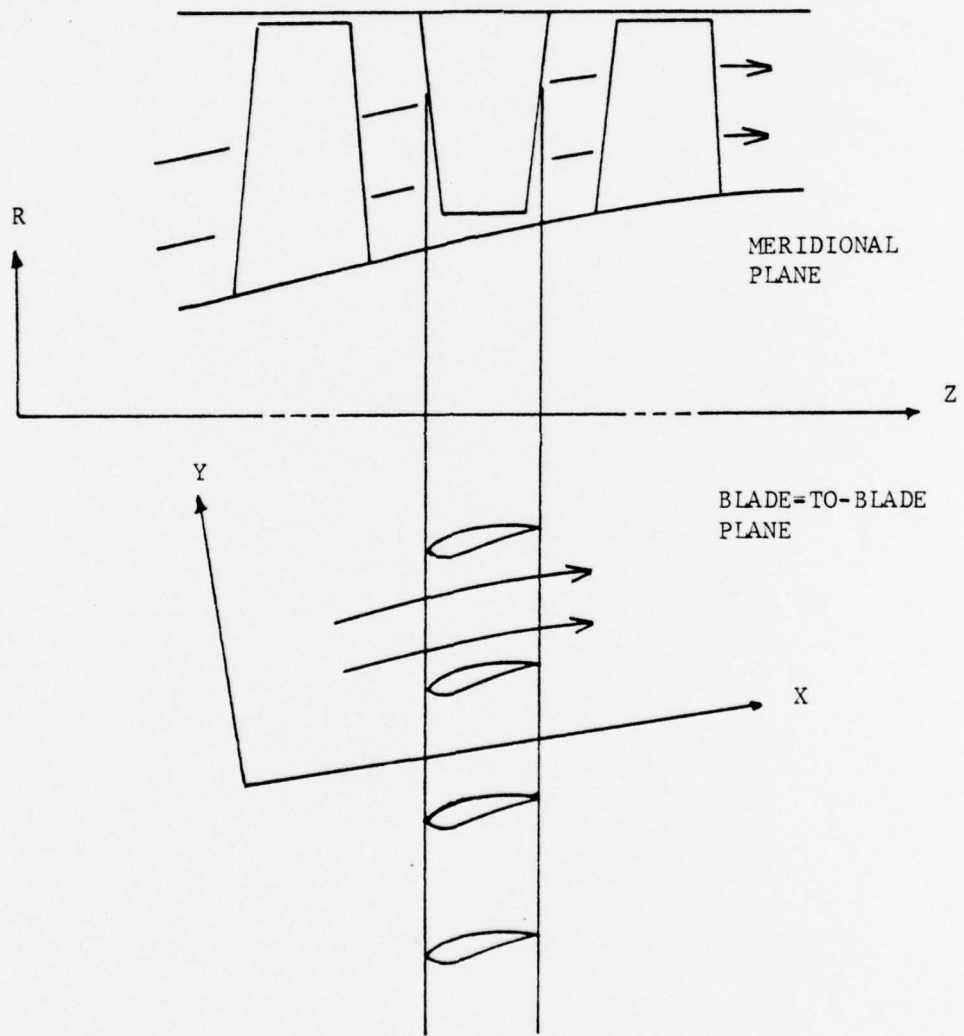


Figure 1 - MERIDIONAL AND BLADE-TO-BLADE PLANES

## II. THEORY

### A. THE DERIVATION OF THE RADIAL EQUILIBRIUM EQUATION

The following discussion is taken from Ref. 7 with slight changes in notation. The basic turbomachine geometry to be analyzed is depicted in Fig 2. Although the machine noted is one stage of a compressor, a similar analysis to the one that follows may be applied to other machines such as axial turbines and mixed-flow machines.

One begins with the Euler equation assuming the viscous forces to be negligible.

$$\frac{d\vec{V}}{dt} + (\vec{V} \cdot \nabla) \vec{V} = \nabla P / \rho \quad (\text{II.A.1})$$

The continuity equation, assuming unsteady flow is,

$$\frac{d\rho}{dt} + \nabla(\rho\vec{V}) = 0 \quad (\text{II.A.2})$$

The First Law of thermodynamics in a fluid field becomes,

$$T \nabla s = \nabla h - \nabla P / \rho \quad (\text{II.A.3})$$

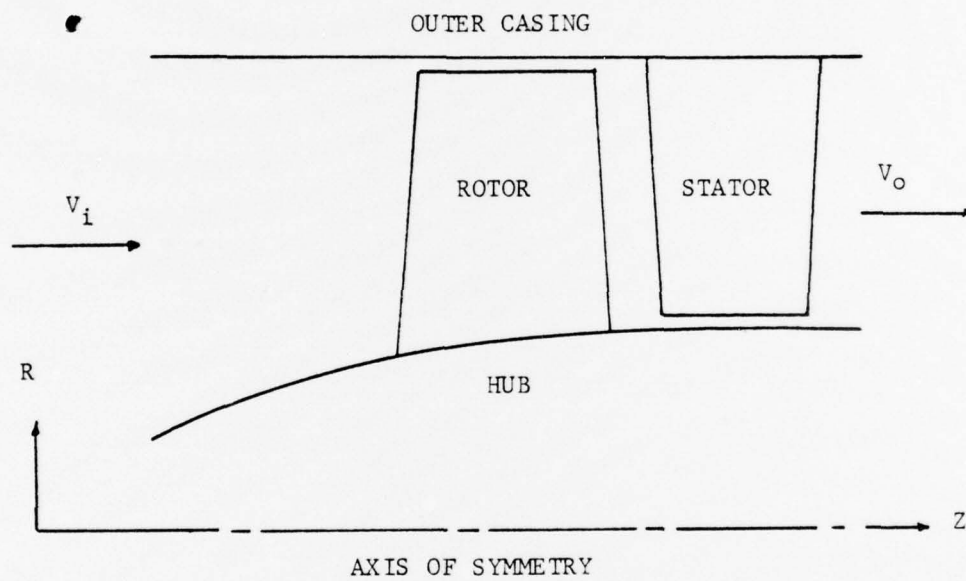


Figure 2 - TURBOMACHINE GEOMETRY

Substituting equation (II.A.3) into equation (II.A.1) leads to the Crocco equation,

$$\frac{d\vec{V}}{dt} - \vec{V} \times (\nabla \times \vec{V}) = T \nabla s - \nabla H \quad (\text{II.A.4})$$

where  $H$  is the total enthalpy.

Assuming a steady and adiabatic flow, the energy equation becomes simply,

$$(\vec{V} \cdot \nabla) H = 0 \quad (\text{II.A.5})$$

which shows that along a streamline in a stationary system, the total enthalpy is constant.

In a relative system, such as the case in a rotor blade row, the total relative velocity,  $\vec{W}$ , can be expressed in the following form,

$$\vec{W} = \vec{V} + \vec{\omega} \times \vec{R} = \vec{V} + \vec{U} \quad (\text{II.A.6})$$

where  $\vec{\omega}$  is the constant angular velocity and  $\vec{U}$  is the constant peripheral speed of the relative system.

Now, the Crocco equation in a relative system becomes,

$$\frac{d\vec{W}}{dt} - \vec{W} \times (\nabla \times \vec{W}) = T \nabla s - \nabla \left( h + \frac{W^2}{2} - \frac{\omega^2 R^2}{2} \right) \quad (\text{II.A.7})$$

Parallel to equation (II.A.5) for the stationary system, the energy equation, assuming steady and adiabatic (relative) flow in a relative system, becomes

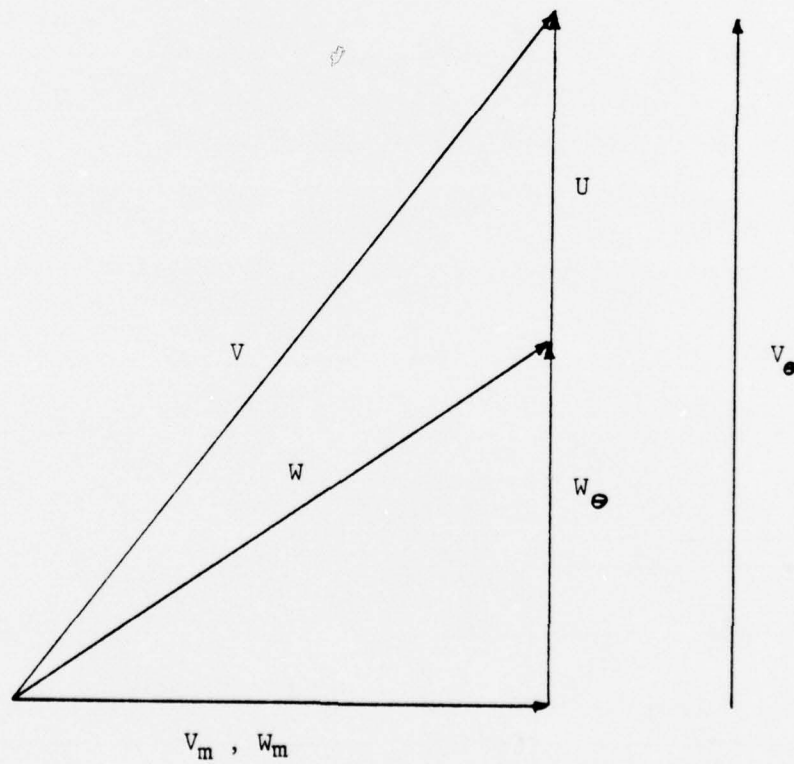
(II.A.8)

$$(\vec{w} \cdot \nabla) H_R = 0$$

where  $H_R$  is the relative total enthalpy expressed as follows,

$$H_R = h + \frac{w^2}{2} - \frac{\omega^2 R^2}{2} \quad \text{(II.A.9)}$$

From the following velocity diagram,



equation (II.A.9) may be arranged as follows.

Since,

$$W_m^2 + W_\theta^2 = W^2 = V_m^2 + (V_\theta - U)^2 \quad (\text{II.A.10})$$

then,

$$W^2 = V_m^2 + V_\theta^2 - 2UV_\theta + U^2 \quad (\text{II.A.11})$$

and,

$$W^2 = V^2 + U^2 - 2UV_\theta \quad (\text{II.A.12})$$

Substituting equation (II.A.12) into equation (II.A.9) leads to the following relation,

$$H_r = h + \frac{V^2}{2} - UV_\theta = H - UV_\theta \quad (\text{II.A.13})$$

Equation (II.A.8) shows that  $H_r$  is constant along a streamline in a relative system.

Upon integrating equation (II.A.8) between the rotor inlet and outlet, the Euler equation for turbomachines is found,

$$\Delta H \Big|_{IN}^{OUT} = \Delta (\vec{U} \cdot \vec{V}_\theta) \Big|_{IN}^{OUT} \quad (\text{II.A.14})$$

It may be shown [Ref.9] that by circumferentially averaging equation (II.A.1), and under the axi symmetric flow assumption the following relation is valid,

$$-\vec{V} \times (\nabla \times \vec{V}) = T \cdot \nabla S - \nabla H + F_b + F_d \quad (\text{II.A.15})$$

where  $F_b$  is the body force of the blades acting on the fluid and all variables are mean values along the direction of the circumference. Hence equation (II.A.15) is an approximation for axi symmetric flow. As a final note on equation (II.A.15), since the viscous forces were neglected in equation (II.A.1), there must be a force introducing the entropy variations along the blade. This force is proportional to the pressure loss coefficient and is labeled  $F_d$ , the dissipative force.  $F_d$  produces work which in turn produces entropy production radially along the blade. Under the axi symmetric assumption, entropy varies axially and radially only and is assumed to be proportional to the pressure loss coefficients [Ref. 2 and 8].

. Due to boundary conditions imposed on the problem and the axi symmetric assumption, cylindrical coordinates,  $(r, \theta, z)$ , will be used in all subsequent analysis. Therefore, equation (II.A.15), in cylindrical coordinates and with axial symmetry is as follows,

$$\frac{V_\theta}{R} \frac{\partial}{\partial R} (R V_\theta) - V_z \left( \frac{\partial}{\partial z} V_r - \frac{\partial}{\partial R} V_z \right) = \frac{\partial H}{\partial R} - T \frac{\partial S}{\partial R} - F_{br} - F_{dr} \quad (\text{II.A.16})$$

$$\frac{V_z}{R} \frac{\partial}{\partial z} (R V_\theta) + \frac{V_r}{R} \frac{\partial}{\partial R} (R V_\theta) = F_\theta \quad (\text{II.A.17})$$

$$V_R \left( \frac{\partial}{\partial z} V_R - \frac{\partial}{\partial R} V_z \right) - \frac{V_\theta}{R} \frac{\partial}{\partial z} (R V_\theta) = \frac{\partial H}{\partial z} - T \frac{\partial s}{\partial z} - F_z \quad (\text{II.A.18})$$

It is important to note here that under the axisymmetric assumptions, equation (II.A.15) reduces to the following,

$$\vec{V} \cdot \vec{F}_b = 0 \quad (\text{II.A.19})$$

Likewise in a relative system (rotor), the axisymmetric assumption leads to the following,

$$\vec{W} \cdot \vec{F}_b = 0 \quad (\text{II.A.20})$$

Equation (II.A.16) describes the meridional through flow radial equilibrium equation for the finite element method. Since one is concerned with the meridional plane, the following derivative expression is taken from Fig 3.

$$V_m \frac{\partial}{\partial m} = V_R \frac{\partial}{\partial R} + V_z \frac{\partial}{\partial z} \quad (\text{II.A.21})$$

Therefore equation (II.A.17) reduces to,

$$R F_\theta = V_m \frac{\partial}{\partial m} (R V_\theta) \quad (\text{II.A.22})$$

which reveals that in a duct where there are no blades and therefore no blade forces, angular momentum is constant

along a streamline. In that case,

$$\frac{d}{dm}(Rv_\theta) = 0 \quad (\text{II.A.23})$$

As shown in Ref.9, the circumferentially averaged continuity equation is the following,

$$\frac{d}{dR}(\rho R b v_R) + \frac{d}{dz}(\rho R b v_z) = 0 \quad (\text{II.A.24})$$

where  $b$  is the blockage factor defined by Hirsch and Warzee as the tangential area reduction due to the thickness of the blade.

$$b = 1 - \frac{t}{s} \quad (\text{II.A.25})$$

where  $t$  is blade thickness and  $s$  is blade spacing.

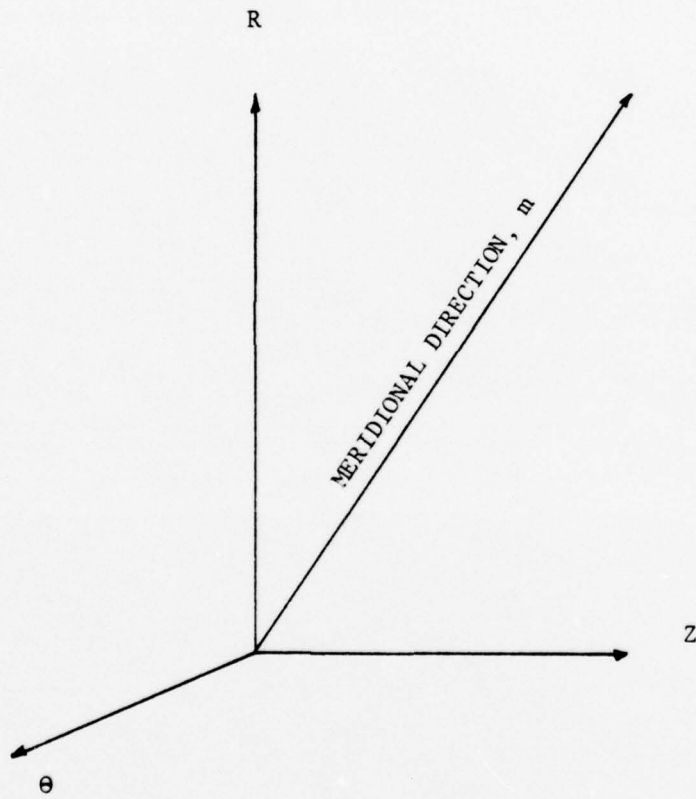


Figure 3 - MERIDIONAL PLANE

One further step in the formulation of the radial equilibrium equation for solution by the finite element method involves introducing the stream function. In cylindrical coordinates, the stream functions are defined as follows,

$$V_z = \frac{1}{\rho R b} \frac{\partial \psi}{\partial R} \quad (\text{II.A.26})$$

$$V_r = - \frac{1}{\rho R b} \frac{\partial \psi}{\partial z} \quad (\text{II.A.27})$$

Substituting these expressions into equation (II.A.16), the equation becomes,

$$\frac{\partial}{\partial R} \left( \frac{1}{\rho R b} \frac{\partial \psi}{\partial R} \right) + \frac{\partial}{\partial z} \left( \frac{1}{\rho R b} \frac{\partial \psi}{\partial z} \right) = \frac{1}{V_z} \left[ \frac{\partial H}{\partial R} - T \frac{\partial s}{\partial R} - \frac{V_\theta}{R} \frac{\partial}{\partial R} (R V_\theta) - F_{br} - F_{dr} \right] \quad (\text{II.A.28})$$

The right hand side of equation (II.A.28) is applicable to the absolute flows in the stator and duct regions. For relative flows such as those in the rotor, the right hand side is modified by replacing the total enthalpy,  $H$ , by the relative total enthalpy,  $H_r$ , and the quantity  $V_\theta/R$  is replaced by  $W_\theta/R$ .

As a last assumption in the formulation of the governing relation for the meridional through flow radial equilibrium equation, both the radial component of the body force,  $F_b$ , and the radial component of the dissipative force,  $F_d$ , are neglected. This assumption, [Ref.1,8] does not hamper the accuracy of the results for conditions at design speed. Even though published compressor performance data used for

the test case in this thesis was obtained at 0.5 design speed, these force terms were also neglected in the computer program. As will be shown later, this assumption could possibly have had adverse effects on the predicted axial velocity profiles at the rotor hub and tip regions.

The final representation of the meridional radial equilibrium equation to be solved by the finite element method is as follows,

$$\frac{d}{dR} \left( k \frac{d\psi}{dR} \right) + \frac{d}{dz} \left( K \frac{d\psi}{dz} \right) + f = 0 \quad (\text{II.A.29})$$

where,

$$k = \frac{1}{\rho R b} \quad (\text{II.A.30})$$

and

$$f = \frac{1}{V_z} \left[ T \frac{ds}{dR} - \frac{dH}{dR} + \frac{V_\theta}{R} \frac{1}{dR} (R V_\theta) \right] \quad (\text{II.A.31})$$

## B. THE FINITE ELEMENT METHOD APPLIED TO THE RADIAL EQUILIBRIUM EQUATION

In order to formulate equations (II.A.29) through (II.A.31) in matrix form for solution by the finite element method, one must apply a weighted residual technique to the equations for numerical solution. The weighted residual method used here is the Galerkin's Method. The following discussion is taken from Ref. 7 with only slight changes in notation.

Rewriting equation (II.A.29) and dividing through by R, one has,

(II.B.1)

$$\frac{1}{R} \left\{ \frac{\partial}{\partial R} \left( K \frac{\partial \psi}{\partial R} \right) + \frac{\partial}{\partial z} \left( K \frac{\partial \psi}{\partial z} \right) + f \right\} = 0$$

where this equation represents the flow in the volume, V.

The boundary condition for this partial differential equation, after dividing through by R, is,

$$\frac{1}{R} \left\{ K \frac{\partial \psi}{\partial n} + \alpha_1 (\psi - \psi_0) \right\} = 0 \quad (\text{II.B.2})$$

where this equation solves the flow on the closed boundary of the volume, or, S.

By applying the weighted residual process to equations (II.B.1) and (II.B.2) and using an arbitrary weighting function, W(r,z), one has

$$\int_V W(r,z) r_{\text{VOL}} dV + \int_S W(r,z) r_{\text{SUR}} dS = 0 \quad (\text{II.B.3})$$

where  $r_{\text{VOL}}$  and  $r_{\text{SUR}}$  are the volume and surface residuals respectively, or,

$$r_{\text{VOL}} = - \frac{1}{R} \left\{ \frac{\partial}{\partial R} \left( K \frac{\partial \psi}{\partial R} \right) + \frac{\partial}{\partial z} \left( K \frac{\partial \psi}{\partial z} \right) + f \right\} = 0 \quad (\text{II.B.4})$$

$$r_{\text{SUR}} = \frac{1}{R} \left\{ K \frac{\partial \psi}{\partial n} + \alpha_1 (\psi - \psi_0) \right\} \quad (\text{II.B.5})$$

If the solution to equation (II.B.1) was exact, both  $r_{\text{VOL}}$  and  $r_{\text{SUR}}$  would be equal to zero.

In order to clarify the boundary condition, equation (II.B.2), one may analyze the equation as follows.

On the surface,  $S$ , where  $\psi$  is specified,

$$\psi = \psi_0 \quad (\text{II.B.6})$$

and,

$$\alpha_1 \rightarrow \infty \quad (\text{II.B.7})$$

Similarly, on the surface, where  $\frac{d\psi}{dn} = 0$ ,  $S_2$ , where

$$\alpha_1 = 0 \quad (\text{II.B.8})$$

$$S_1 \cap S_2 = 0, \quad S_1 \cup S_2 = S \quad (\text{II.B.9})$$

Due to the axi symmetric assumption, the final equation will not involve  $dV$  and  $dS$  but the intersection of  $dV$  and  $dS$  with the meridional plane. Therefore, one must transform the volume integral,  $dV$ , to a surface integral and the surface integral,  $dS$ , to a line integral.

Hence, let,

$d\Omega$  = intersection of  $dV$  and meridional plane

$dC$  = intersection of  $dS$  and meridional plane

and,

$$dV = 2\pi R d\Omega$$

$$dS = 2\pi R dC$$

With this transformation, one may rewrite equation

(II.B.3) as follows,

$$\int_{\Omega} -W(R,z) \left[ \frac{\partial}{\partial R} \left( K \frac{\partial \psi}{\partial R} \right) + \frac{\partial}{\partial z} \left( K \frac{\partial \psi}{\partial z} \right) + f \right] 2\pi d\Omega + \int_C W(R,z) K \frac{\partial \psi}{\partial n} 2\pi dC = 0 \quad (\text{II.B.10})$$

where on the contour,  $q, \psi = \psi_0$ .

One must now integrate the first term in equation (II.B.10) by parts to obtain the following,

$$\begin{aligned} & - \int_{\Omega} W \left[ \frac{\partial}{\partial R} \left( K \frac{\partial \psi}{\partial R} \right) + \frac{\partial}{\partial z} \left( K \frac{\partial \psi}{\partial z} \right) \right] 2\pi d\Omega - \int_{\Omega} W \cdot f d\Omega \\ & + \int_{\Omega} K \left[ \frac{\partial \psi}{\partial R} \frac{\partial W}{\partial R} + \frac{\partial \psi}{\partial z} \frac{\partial W}{\partial z} \right] d\Omega + \int_C W K \frac{\partial \psi}{\partial n} 2\pi dC = 0 \end{aligned} \quad (\text{II.B.11})$$

Inspecting the first term in equation (II.B.11), one may use the following integral theorem to simplify further

$$\int_{\Omega} \partial_{\beta} \phi d\Omega = \int_C \phi n_{\beta} dC \quad (\text{II.B.12})$$

Rewriting equation (II.B.11) gives,

$$\begin{aligned} & - \int_C W K \left[ \frac{\partial \psi}{\partial R} n_R + \frac{\partial \psi}{\partial z} n_z \right] dC - \int_{\Omega} W f d\Omega + \int_{\Omega} K \left[ \frac{\partial \psi}{\partial R} \frac{\partial W}{\partial R} + \frac{\partial \psi}{\partial z} \frac{\partial W}{\partial z} \right] d\Omega \\ & + \int_C W K \frac{\partial \psi}{\partial n} 2\pi dC = 0 \end{aligned} \quad (\text{II.B.13})$$

Finally, since

$$\frac{\partial \psi}{\partial n} = \frac{\partial \psi}{\partial R} n_R + \frac{\partial \psi}{\partial z} n_z \quad (\text{II.B.14})$$

equation (II.B.13) reduces to the following,

$$\int_{\Omega} \left[ K \left( \frac{\partial \Psi}{\partial R} \frac{\partial W}{\partial R} + \frac{\partial \Psi}{\partial z} \frac{\partial W}{\partial z} \right) - fW \right] d\Omega = 0 \quad (\text{II.B.15})$$

One now has the final equation in the form for use by the weighted residual method using any arbitrary weighting function,  $W(r,z)$ . As noted previously, the Galerkin's Method will be used here which implies that the weighting functions are the same functions used in approximating the stream function,  $\Psi$ .

Before applying the finite element method, one must discretize the continuum and then approximate the unknown function,  $\Psi$ , by a set of polynomials. For this particular problem, eight-noded iso-parametric elements were chosen for discretization, see Fig 4, and the following approximating functions were used.

$$\Psi = \sum_{i=1}^8 N_i(\xi, \eta) \Psi_i \quad (\text{II.B.16})$$

where,

$N_i(\xi, \eta)$  = shape functions

$\Psi_i$  = value of  $\Psi$  at the node

$\Psi$  = value of  $\Psi$  at any arbitrary location within the element. The shape functions,  $N_i$ , used here are defined by the following relations as shown in Ref.10,

$$N_i(\xi, \eta) = \frac{1}{4}(1 + \xi\xi_i)(1 + \eta\eta_i)(\xi\xi_i + \eta\eta_i - 1)$$

$$N_i(\xi, \eta) = \frac{1}{2}(1 - \xi^2)(1 + \eta\eta_i) \quad (\text{II.B.17})$$

$$N_i(\xi, \eta) = \frac{1}{2}(1 + \xi\xi_i)(1 - \eta^2)$$

where the following coordinate transformations are used,

$$r = \sum_{i=1}^8 N_i(\xi, \eta) r_i \quad (\text{II.B.18})$$

$$z = \sum_{i=1}^8 N_i(\xi, \eta) z_i$$

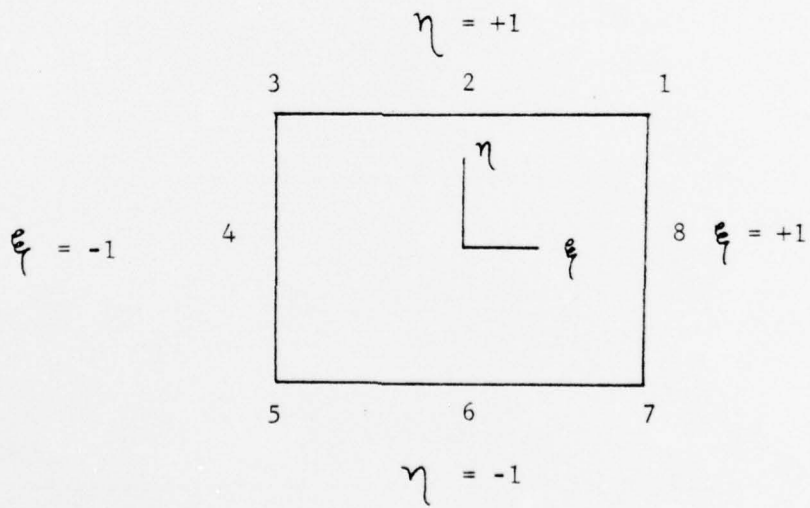
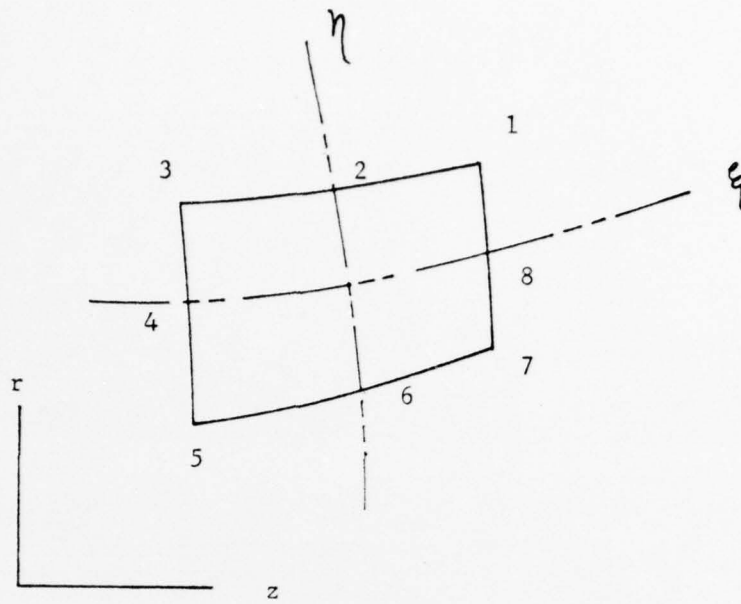


Figure 4 - ISOPARAMETRIC QUADRILATERAL ELEMENT

At this point, one is ready to apply the Galerkin Method to equation (II.B.15) by substituting equation (II.B.16) for the unknown function  $\Psi$ , and  $N_i$  for the weight function,  $w$ , which yields,

$$\int_{\Omega} k \left\{ \frac{\partial N_i}{\partial r} \sum_{j=1}^8 \Psi_j \left( \frac{\partial N_j}{\partial r} \right) + \frac{\partial N_i}{\partial z} \sum_{j=1}^8 \Psi_j \left( \frac{\partial N_j}{\partial z} \right) \right\} d\Omega - \int_{\Omega} f_i N_i d\Omega = 0 \quad (\text{II.B.19})$$

This integration yields the following system of equations which is solved for the unknown nodal  $\Psi$ ,

$$\begin{bmatrix} K_{11} & K_{12} & \cdots & K_{1n} \\ \vdots & & & \\ K_{n1} & \cdots & & K_{nn} \end{bmatrix} \begin{Bmatrix} \Psi_1 \\ \vdots \\ \Psi_n \end{Bmatrix} = \begin{Bmatrix} f_1 \\ \vdots \\ f_n \end{Bmatrix} \quad (\text{II.B.20})$$

where,

$$K_{ij} = \int_{\Omega} k \left\{ \frac{\partial N_i}{\partial r} \frac{\partial N_j}{\partial r} + \frac{\partial N_i}{\partial z} \frac{\partial N_j}{\partial z} \right\} d\Omega \quad (\text{II.B.21})$$

and,

$$f_i = \int_{\Omega} f \cdot N_i d\Omega \quad (\text{II.B.22})$$

In addition since both the 'stiffness matrix',  $K$ , and the right hand side vector,  $[F]$ , are functions of  $\Psi$ , the system as defined by equations (II.B.20) through (II.B.21) must be solved iteratively.

At this point one has the total finite element formulation of the radial equilibrium equation as defined by equations (II.B.19) and (II.B.20). The problems which remain to be clarified are basically two fold. Firstly one

must evaluate the integrals in equations (II.B.19) and (II.B.2) by numerical methods, and secondly, the solution procedure for the non-linearity must be formulated. In Part C, both of these final steps are presented.

### C. NUMERICAL INTEGRATION OF STIFFNESS MATRIX AND SOLUTION PROCEDURE

#### 1. Numerical integration of the stiffness matrix

As noted in Section II.B, evaluation of equation (II.B.21) must be performed numerically. In addition, one realizes that the derivative expressions enclosed within the interval must be evaluated by a coordinate transformation. This is done in the following way,

Since,

$$r = \sum_{i=1}^8 N_i(\xi, \eta) r_i \quad (II.C.1)$$

$$z = \sum_{i=1}^8 N_i(\xi, \eta) z_i$$

then,

$$\frac{\partial N_i}{\partial \xi} = \frac{\partial N_i}{\partial z} \frac{\partial z}{\partial \xi} + \frac{\partial N_i}{\partial r} \frac{\partial r}{\partial \xi} \quad (II.C.2)$$

$$\frac{\partial N_i}{\partial \eta} = \frac{\partial N_i}{\partial z} \frac{\partial z}{\partial \eta} + \frac{\partial N_i}{\partial r} \frac{\partial r}{\partial \eta}$$

and in matrix form,

$$\begin{pmatrix} \frac{\partial N_i}{\partial \xi} \\ \frac{\partial N_i}{\partial \eta} \end{pmatrix} = \begin{bmatrix} \frac{\partial z}{\partial \xi} & \frac{\partial r}{\partial \xi} \\ \frac{\partial z}{\partial \eta} & \frac{\partial r}{\partial \eta} \end{bmatrix} \begin{pmatrix} \frac{\partial N_i}{\partial z} \\ \frac{\partial N_i}{\partial r} \end{pmatrix} \quad (\text{II.C.3})$$

Furthermore, defining the Jacobian matrix as,

$$J = \begin{bmatrix} \frac{\partial z}{\partial \xi} & \frac{\partial r}{\partial \xi} \\ \frac{\partial z}{\partial \eta} & \frac{\partial r}{\partial \eta} \end{bmatrix} \quad (\text{II.C.4})$$

then by dividing both sides of equation (II.C.3) by  $J$ , one has the following transformation,

$$\begin{pmatrix} \frac{\partial N_i}{\partial z} \\ \frac{\partial N_i}{\partial r} \end{pmatrix} = [J]^{-1} \begin{pmatrix} \frac{\partial N_i}{\partial \xi} \\ \frac{\partial N_i}{\partial \eta} \end{pmatrix} \quad (\text{II.C.5})$$

In addition, it has been shown [Ref.9] that

$$dzdr = |J| d\xi d\eta \quad (\text{II.C.6})$$

Now, with equations (II.C.5) and (II.C.6), equation (II.B.21) becomes the following,

$$K_{ij} = \int_{-1}^1 \int_{-1}^1 k \left[ \frac{\partial N_i}{\partial \xi} \frac{\partial N_j}{\partial \eta} \right] \{ [J]^{-1} \}^T [J]^{-1} \begin{Bmatrix} \frac{\partial N_i}{\partial \xi} \\ \frac{\partial N_j}{\partial \eta} \end{Bmatrix} \det [J] d\xi d\eta \quad (\text{II.C.7})$$

Equation (II.C.7) is best integrated using the Gauss-Legendre integration method since it is of the following form,

$$K_{ij} = \int_{-1}^1 \int_{-1}^1 G(\xi, \eta) d\xi d\eta \quad (\text{II.C.8})$$

or finally, [Ref.10],

$$K_{ij} = \sum_{i=1}^2 \{ A_i B_i f(\xi_i, \eta_i) \} \quad (\text{II.C.9})$$

where  $A_i$  and  $B_i$  are coefficients (Fig 5) for both two and three point Gaussian Quadrature.

At this point, one has the tools to calculate all the elements of the stiffness matrix. In like manner, the right hand side vector,  $f$ , is calculated by numerical integration.

NUMBER OF GAUSSIAN POINTS	$\pm \eta$ $\pm \xi$	$\pm A_i$ $\pm B_i$
2	0.57735 02691	1.00000 00000
3	0.77459 66692 0.00000 00000	0.55555 55555 0.88888 88888

Figure 5 - GAUSSIAN INTEGRATION POINTS

## 2. Solution procedure

The following is a synopsis of the basic solution process. Specific details concerning equations and methods of computer coding are covered in the proceeding section. The proceeding is meant to give the reader a preview of the solution process.

### a. Discretization

Initially the machine under analysis is discretized into eight-node iso-parametric elements. The axial calculation stations are placed arbitrarily in the duct regions and along blade edges and centers for the rotor and stator as shown in Fig 6. At this point the system topology and nodal coordinates are specified.

### b. Initialization

To begin the iteration process, one must assume an initial internal stream function, velocity, and density distribution. In the program, the initial internal stream function was assumed to be that of the outer boundary throughout while the velocity and density distribution was assumed to be that of the inlet.

CAVITTO NASA TASK 1

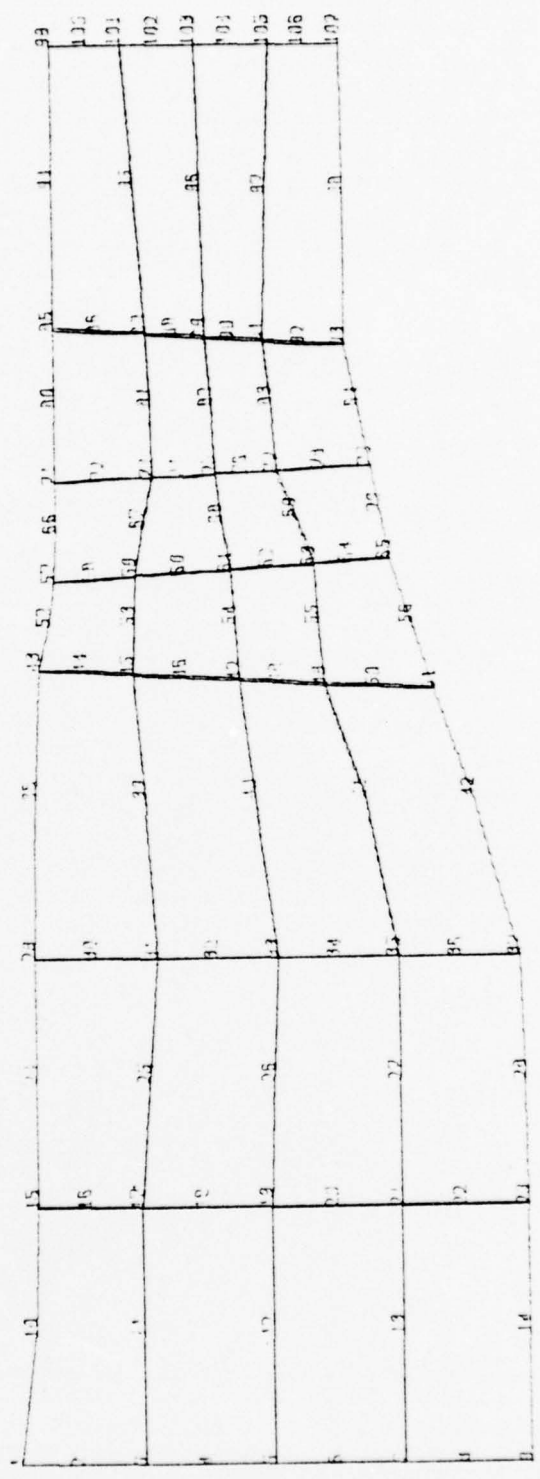


Figure 6 - COMPRESSOR DISCRETIZATION

c. Calculation of thermodynamic variables

Before calculating the right-hand side vector,  $f$ , one must obtain distributions of angular momentum, enthalpy, and entropy. This is done by first calculating the thermodynamic variables at the inlet axial station from the given inlet conditions. In order to proceed axially through the machine to calculate the nodal angular momentum, enthalpy, and entropy, the following three equations derived in Section III are used.

$$H = C_p T = \text{constant along a stator streamline}$$

$$H_R = C_p T_r - \frac{(w_r)^2}{2} = \text{constant along a rotor streamline}$$

$$r V_\theta = \text{constant along a duct streamline}$$

An example of this calculation procedure for the duct region is shown graphically in Fig 7.

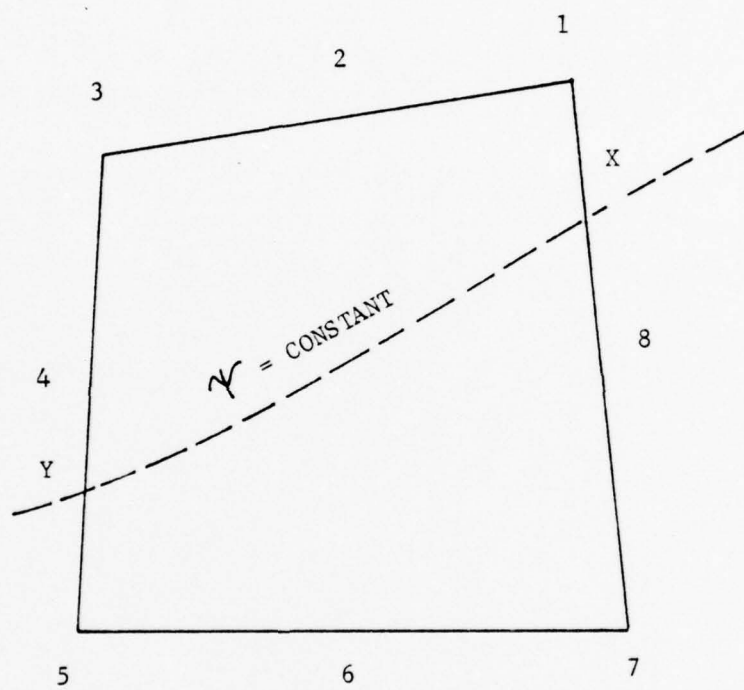


Figure 7 - DUCT ELEMENT

In this figure, the angular momentum at point X is equal to the angular momentum at point Y. More formally,

$$(rV_{\theta})_X = \sum_{i=3}^5 N_i(\xi, \eta) (rV_{\theta})_i = (rV_{\theta})_Y \quad (\text{II.C.2.1})$$

Since the previous axial station's thermodynamic variables are known, one must now find the values of  $\xi$  and  $\eta$  at point Y. This is done iteratively in the following way. Since

$$\psi|_Y = \psi|_X = \sum_{i=3}^5 N_i(\xi, \eta) \psi_i \quad (\text{II.C.2.2})$$

and along the left side of the element,

$$\xi = -1 \quad (\text{II.C.2.3})$$

then equation (II.C.2.2) may be solved for  $\eta$  by a suitable iteration method. As will be shown in the next section, a half-interval method was used to obtain the unknown  $\eta$ . Once  $\eta$  is known, then equation (II.C.2.1) is solved for the angular momentum at point X. The rotor and stator are handled in a similar fashion. In addition, the rotor and stator deviate the flow creating a three-dimensional flow field between the blades in the respective blade row. Low speed cascade correlation data [Ref.13] was used to calculate the effective turning angles in the rotor and stator. These effects are calculated beforehand with known mass flow rate and uniform axial velocity assumptions at the rotor inlet. The results of these calculations are part of the input data routine in the form of relative and absolute flow angles at the rotor nodes and absolute flow angles at

the stator nodes. This will be shown more exactly in the next section.

d. Calculate matrices

At this point, the right hand side vector,  $f$ , and the stiffness matrix,  $K$ , are calculated.

e. Solve system of equations

The system of equations as shown in equation (II.B.20) is solved for the nodal stream function.

f. Perform relaxation iteration

Due to the strong non-linear properties of the system of equations, the following iterative scheme is necessary.

$$\psi_i^{n+1} = \psi_i^n + \alpha [\hat{\psi}_i^{n+1} - \psi_i^n] \quad (\text{II.C.2.4})$$

where  $\alpha$  is the under relaxation factor. As will be shown in Section III, this scheme is performed only in certain regions of the machine and in addition after a specified number of iterations.

g. Update velocity and density profiles

Using the current nodal distribution of the stream function, axial and radial nodal velocity components are calculated along with a new nodal density distribution.

Again, this calculation procedure will be shown in the next section.

h. Test for convergence of  $\psi$

Stream function convergence criteria is now tested and will determine if further iterations are necessary. The solution is said to converge if the following equation holds for all nodes.

$$\left| \frac{\psi_i^n - \psi_i^{n+1}}{\psi_i^{n+1}} \right| < \epsilon \quad (\text{II.C.2.5})$$

where  $\epsilon$  is a designated requirement for convergence.

i. Summary

In summary, the eight steps involved in the solution are noted below;

- (1) Discretize the continuum.
- (2) Assume an initial stream function, velocity, and density solution.
- (3) Calculate the nodal thermodynamic variables from the given inlet conditions.
- (4) Form the right hand side vector,  $f(r,z)$ , and the stiffness matrix,  $K$ .
- (5) Solve the system of equations, given by,  $[K] = [F]$  for a new stream function distribution.

(6) Perform relaxation iteration if required.

(7) Calculate new nodal velocity and density distributions from the current stream function solution.

(8) Test the solution for convergence, and if required, repeat steps (3) through (8) using the current nodal stream function values.

This concludes the solution description and now one is ready to more completely understand the computer program which assembles the preceding eight steps.

### III. THE PROGRAM

#### A. OVERALL FLOWCHART AND DESCRIPTION

The overall flowchart of the program is depicted in Fig 8. Those blocks denoted by the letter 'S' are subroutines, while the remaining calculations are an integral part of the main program.

After proper dimensioning of all arrays and subsequent initialization, the input data are read and then printed. This not only presents a physical picture of the problem but also serves as a cross check to the user for correct data insertion. In addition, a subroutine is available to obtain a computer drawn plot of the mesh (Fig 6) and is a further check on proper data input.

At this point all the necessary variables have been stored and the iteration counter for stream function convergence is set. With the current nodal values of  $\psi$  and the given inlet thermodynamic conditions, the thermodynamic variables throughout the machine are calculated. From the calculated values of enthalpy and angular momentum, (isentropic flow is assumed), the right-hand side vector is calculated followed by the stiffness matrix calculation (equation II.B.21).

The system of equations (equation (II.B.20)) is now solved for the new nodal stream function distribution. It is here where for all iterations but the first that a

relaxation factor is applied as noted previously in equation (II.C.2.4). The reasoning behind not applying the relaxation scheme to the value of nodal  $\Psi$  after the first iteration is the fact that the first iteration produced a close approximation to the correct stream function distribution. With this close approximation to the stream function came a velocity and density distribution which in turn was near the correct solution. It was found that if the first iteration was relaxed, the second iteration became unstable since in fact the velocities and densities were themselves farther from the true values than were assumed initially.

After testing the nodal stream function for convergence by use of equation (II.C.2.5), the calculation process is either repeated or ceased by virtue of convergence or limiting the number of iterations.

As stated previously, low speed cascade correlation data [Ref.13] were used to calculate turning angles in the blade regions. These angles were assumed constant throughout the solution and not refined after subsequent iterations. Further work on the computer program could entail an additional computational routine which would calculate the new turning angles after each iteration. A sample calculation of rotor turning angles is shown in Appendix D.

In the following sections the program structure is examined in more detail.

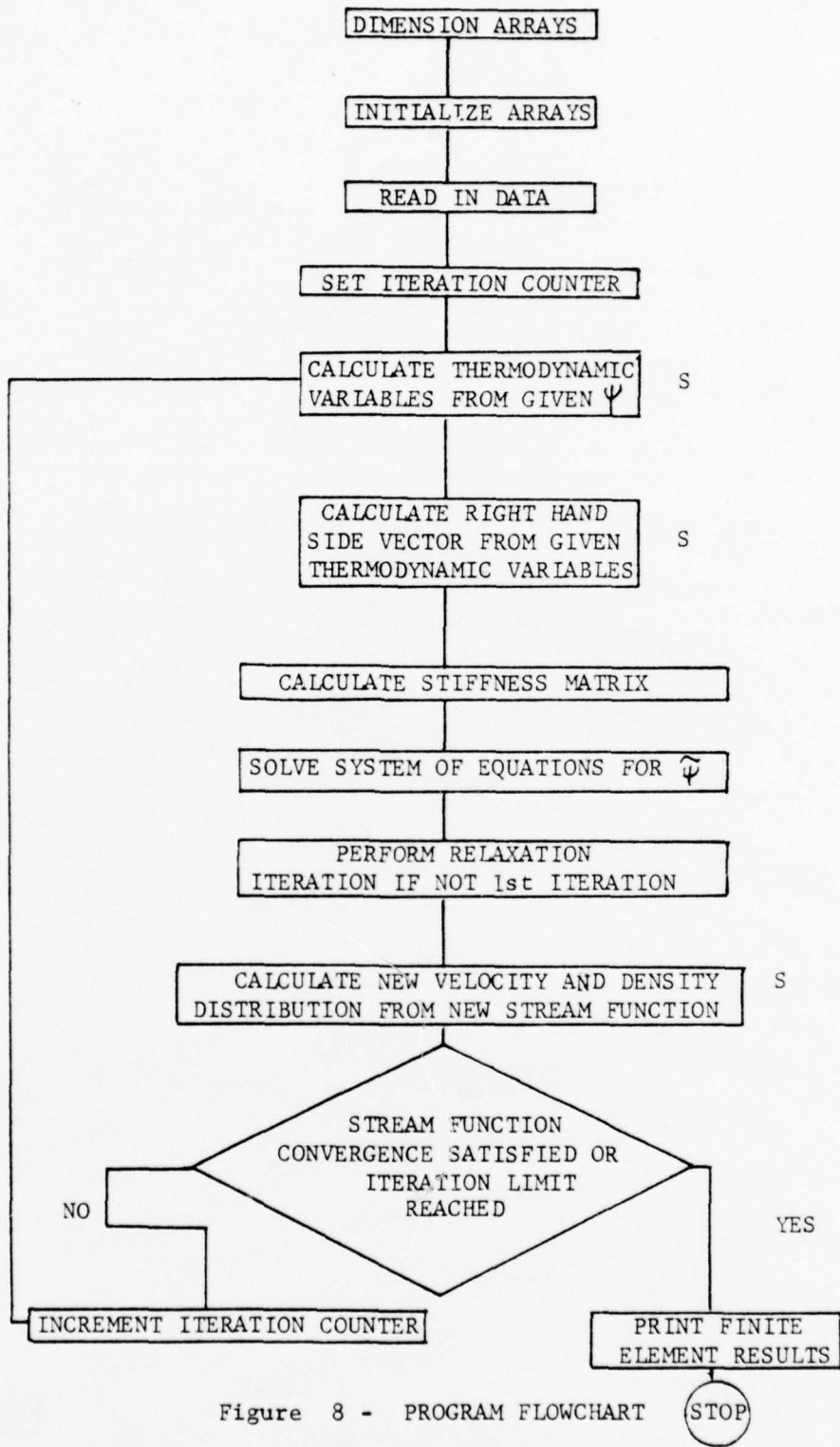


Figure 8 - PROGRAM FLOWCHART

## B. THE MAIN PROGRAM

### 1. The input routine

The following is a description of the input data required by the program. The data are arranged into twelve categories described in the following manner.

#### a. category 1

Problem identification.

#### b. category 2

Number of nodes and number of elements.

#### c. category 3

Node numbers, nodal coordinates and nodal blockage factor.

#### d. category 4

System topology.

#### e. category 5

Element type; duct, rotor, or stator.

f. category 6

Absolute flow angles for rotor and stator nodes.

g. category 7

Relative flow angles for rotor nodes.

h. category 8

Inlet thermodynamic quantities.

i. category 9

Physical constants for fluid under observation.

j. category 10

First estimate of internal stream function.

k. category 11

Node numbers and specified nodal stream function.

l. category 12

Node numbers where the right hand side,  $f(r,z)$ , is to be calculated.

Before describing in detail the format to be followed for data insertion, it is important to note the following assumptions.

(1) Uniform flow conditions at inlet and outlet.

(2) Uniform flow conditions at rotor inlet for calculation of appropriate turning angles. This assumption is necessary to calculate the values of rotor and stator flow angles.

With this in mind, the discussion will continue.

The following describes each category in more detail.

Category 1:

Format: (20A4)

Number of cards: 1

Procedure: Enter the title of the problem in columns 1-20.

Category 2:

Format: (2I10)

Number of cards: Equal to the number of nodes in the system.

Procedure: Enter the number of nodes in columns 1-10, and the number of elements in 11-20. Both integers must be right justified.

Category 3:

Format: (I10,3F10.0)

Number of cards: Equal to the number of nodes in the system.

Procedure: Each card contains the node number followed by the Z coordinate, R coordinate, and nodal blockage factor. The coordinates are in dimensions of inches.

Category 4:

Format: (9I5)

Number of cards: Equal to the number of elements in the system.

Procedure: Each card contains nine integers right justified in columns 5, 10, 15, etc., through 45. The first integer is the element number followed by the eight nodes associated with that element. It is important to note that the nodes are read in starting with the upper right hand node and proceeding in a counterclockwise fashion around the element.

Category 5:

Format: (2I10)

Number of cards: Equal to the number of

elements.

Procedure: Enter the element number in columns 1-10, followed by the integer '1' (duct), '2' (rotor), or '3' (stator) describing the element as either in a duct, rotor, or stator region.

Category 6:

Format: (6X,A4,I10,F10.0)

Number of cards: Equal to the number of rotor and stator nodes plus one 'STOP' card.

Procedure: Enter the node number (right justified) in columns 11-20 followed by the value of the associated absolute flow angle in radians in columns 21-30. The last card in this category is a 'STOP' card entered in columns 7-10.

Category 7:

Format: (6X,A4,I10,F10.0)

Number of cards: Equal to the number of rotor nodes plus one 'STOP' card.

Procedure: Enter the node number (right justified) in columns 11-20 followed by the value of the associated relative flow angle in radians in columns 21-30. The last card in this category is a 'STOP' card.

Category 8:

Format: (7F10.0), (F10.0)

Number of cards: 2

Procedure: Enter the following quantities in the prescribed order and with the noted dimensions.

First card

Mass flow rate: (lbm/sec)

Inlet axial velocity: (ft/sec)

Outlet axial velocity: (ft/sec)

Inlet total density: (lbm/ft<sup>3</sup>)

Inlet static density: (lbm/ft<sup>3</sup>)

Inlet total pressure: (lbf/in<sup>2</sup>)

Inlet total temperature: (°R)

Second card

Speed: (RPM)

Category 9:

Format: (3F10.0)

Number of cards: 1

Procedure: Enter the following quantities in the prescribed order.

Gas constant: (ft-lbf/lbm-°R)

Ratio of specific heats

Constant pressure specific heat:  
(BTU/lbm-°R)

Category 10:

Format: (F10.0)

Number of cards: 1

Procedure: Enter the first estimate of the internal stream function to be used in the first iteration.

Category 11:

Format: (6X,A4,I10,F10.0)

Number of cards: Equal to the number of nodes having a specified value of the stream function plus a 'STOP' card.

Procedure: This set of cards allows the stream function boundary conditions to be read in. A typical card contains an integer, right justified in columns 11-20, which is the node number, followed by the value of the specified stream function in columns 21-30. The last card is a 'STOP' card.

Category 12:

Format: (6X,A4,I10)

Number of cards: Equal to the number of nodes where the right hand side is to be specified.

Procedure: Enter the node number, right justified in columns 11-20, where the right hand side is to be calculated. Again, the last card in this category is a 'STOP' card.

After all the data has been read by the program, the input data is printed and the mesh is plotted for verification by the user. The sample format is shown in Appendix C.

This concludes the input routine. The next section describes the calculation of the stiffness matrix, K.

## 2. Stiffness matrix evaluation

As shown previously in Section II.C.1, the following equation describes each term in the eight by eight elemental matrix.

$$K_{ij} = \int_{-1}^1 \int_{-1}^1 k \left[ \frac{\partial N_i}{\partial \xi} \quad \frac{\partial N_i}{\partial \eta} \right] \{ [J]^{-1} \}^T \{ \} \det [J] d\xi d\eta \quad (\text{III.B.2.1})$$

In addition, 'k' is defined in the following way in order to numerically integrate the equation.

$$k = \frac{1}{\sum_{i=1}^8 p_i N_i(\xi, \eta) \cdot \sum_{i=1}^8 r_i N_i(\xi, \eta) \cdot \bar{b}} \quad (\text{III.B.2.2})$$

where b is defined as the elemental blockage factor taken as an average over the eight nodes of the particular element and  $(\xi, \eta)$  are the defined Gauss-quadrature integration points.

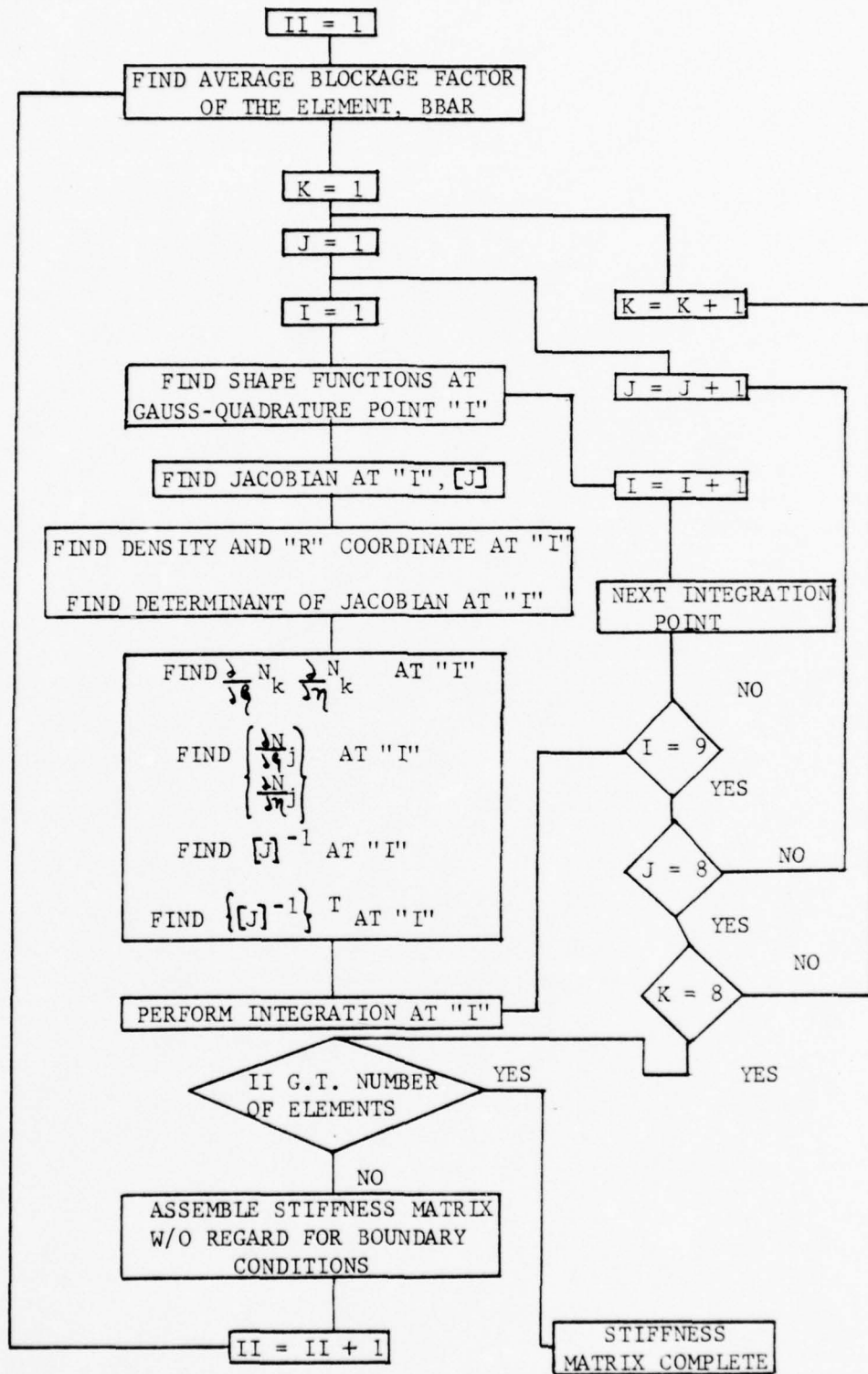


Figure 9 - STIFFNESS MATRIX EVALUATION

Fig 9 depicts the flowchart for both elemental stiffness matrix evaluation and the assemblage into the system stiffness matrix. More specifically, the figure shows a three-point Gaussian Quadrature scheme but can be changed to a two-point scheme by simply integrating four times instead of nine as shown.

The actual coding of the stiffness matrix evaluation and assemblage may be found in lines STR03510 through STR04770 in the computer program.

### 3. Solution of systems of equations

At this point, the system of equations are modified for the boundary conditions and solved for the nodal stream function values. An equation solving routine, DSIMQ, available in the system library was used for this purpose. It was found that no comparable savings was realised by using a banded equation solver.

### 4. Iteration schemes

As noted previously in Section II.C, a relaxation scheme is necessary for convergence to a solution.

Two distinct differences with regard to the iteration method were noted from that of Ref.7. Firstly, it was found that relaxation was necessary only in the rotor and stator elements and also in the duct region between the rotor outlet and stator inlet. Secondly, due to the extreme non linearity in the rotor-stator areas, a switch was required which changed the sign of  $\alpha$  in equation (II.C.2.4) as required for stability of convergence. Clarification of

this change follows: It was found that during the initial three or four iterations, the stream function values of the rotor-stator nodes sometimes exceeded the value of the upper boundary. Due to an absence of sources within the domain of solution, this occurrence was incompatible with the boundary conditions. At this point, it was necessary to make  $\alpha$  negative in equation (II.C.2.4). During subsequent iterations, as the solution converged, the rotor-stator regions became stable and the sign of  $\alpha$  was returned to its positive value. This iteration proved to stabilize the solution with respect to stream function values and velocities.

The iteration procedure is coded in the computer program from lines STR05070 through STR05200.

#### 5. The output routine

Once convergence is obtained or the number of iterations have reached the limit imposed by the user, the results are displayed. A sample output is shown in the Appendix. In addition, the units of all dependent variables are the same as those noted in the input routine.

#### C. THE SUBROUTINES

The following describes each of the six subroutines in the computer program. Each subsection contains a list of calling arguments and for subroutines PCAL, SLINE, and VEL, a basic flowchart. In addition, for those subroutines whose mathematical theory was not presented in Section III, a brief treatment is also given.

1. Subroutine shape

This subroutine calculates the shape functions (equation (II.B.17)) at the values of  $\xi$  and  $\eta$  as requested in the argument list below.

SUBROUTINE SHAPE (E,Z,SP)

E = value of  $\xi$  (input)

Z = value of  $\eta$  (input)

SP = eight by one vector of the eight shape functions.

2. Subroutine jacob

JACOB calculates the Jacobian matrix as defined in equation (II.C.1.4) for the value of  $\xi, \eta$  denoted in the argument list.

SUBROUTINE JACOB (E1,Z1,D,E,RC\$,ZC\$,RJAC)

E1 = value of  $\eta$  (input)

Z1 = value of  $\xi$  (input)

D = eight by one vector of  $\frac{\partial N_i}{\partial \xi}$  (calculated)

E = eight by one vector of  $\frac{\partial N_i}{\partial \eta}$  (calculated)

RC\$ = eight by one vector of the 'r' coordinates of the nodes associated with the element (input)

ZC\$ = eight by one vector of the 'z' coordinates of the nodes associated with the element (input)

RJAC = two by two Jacobian matrix (output)

In addition, the subroutine assumes that the vectors RC\$ and ZC\$ contain element coordinates arranged in a counter clockwise fashion beginning with the upper right corner node.

### 3. Subroutine sline

This subroutine calculates the thermodynamic variables throughout the machine given the inlet conditions as described in Section II.C.2. The calling arguments are defined below.

```
SUBROUTINE SLINE(UINLET,RC,PSI,WRL,H,UVEL,VVEL,TVEL,  
NODE,NNODEI,CP,TT,KK,ALP,WG,TWEL,BE,HS)
```

UINLET = Inlet axial velocity

RC = Nodal 'r' coordinates vector

PSI = Nodal stream function vector

WRL = Nodal angular momentum vector

H = Nodal total enthalpy vector

UVEL = Nodal axial velocity vector

VVEL = Nodal radial velocity vector

TVEL = Nodal absolute tangential velocity vector

NODE = Matrix containing nodes associated with the element

INLET = Vector containing node numbers at inlet station

NNODEI = Number of nodes at inlet station

CP = Specific heat

TT = Total temperature at inlet

KK = Iteration counter  
NTE = Element type vector  
ALP = Nodal absolute flow angle vector  
TWEL = Nodal relative tangential velocity vector  
BE = Nodal relative flow angle vector  
HS = Nodal static enthalpy vector

As shown in Fig 10, the basic calculation procedure begins with calculating the required energy and momentum values at the inlet station. At this point, beginning with element one, the element type is interrogated to distinguish between duct, rotor, and stator elements. If the element is in a duct region, then the streamline intersections for local nodes 2,6,7,8 and 1 (Fig 7) are determined along with the associated values of energy and angular momentum. For the rotor and stator elements, one must initially find the energy and momentum values at local nodes 3,4,5 (Fig 7) due to the discontinuities imposed by the blade edges. Once these calculations are performed, then the process for the remaining nodes in the element proceeds in a similar fashion to the duct elements.

After all the elements have been cycled through, the new distributions of nodal angular momentum and energy are returned to the main program for further computations. Specifically, these values will be used by the next subroutine, FCAL, for calculation of the right hand side vector.

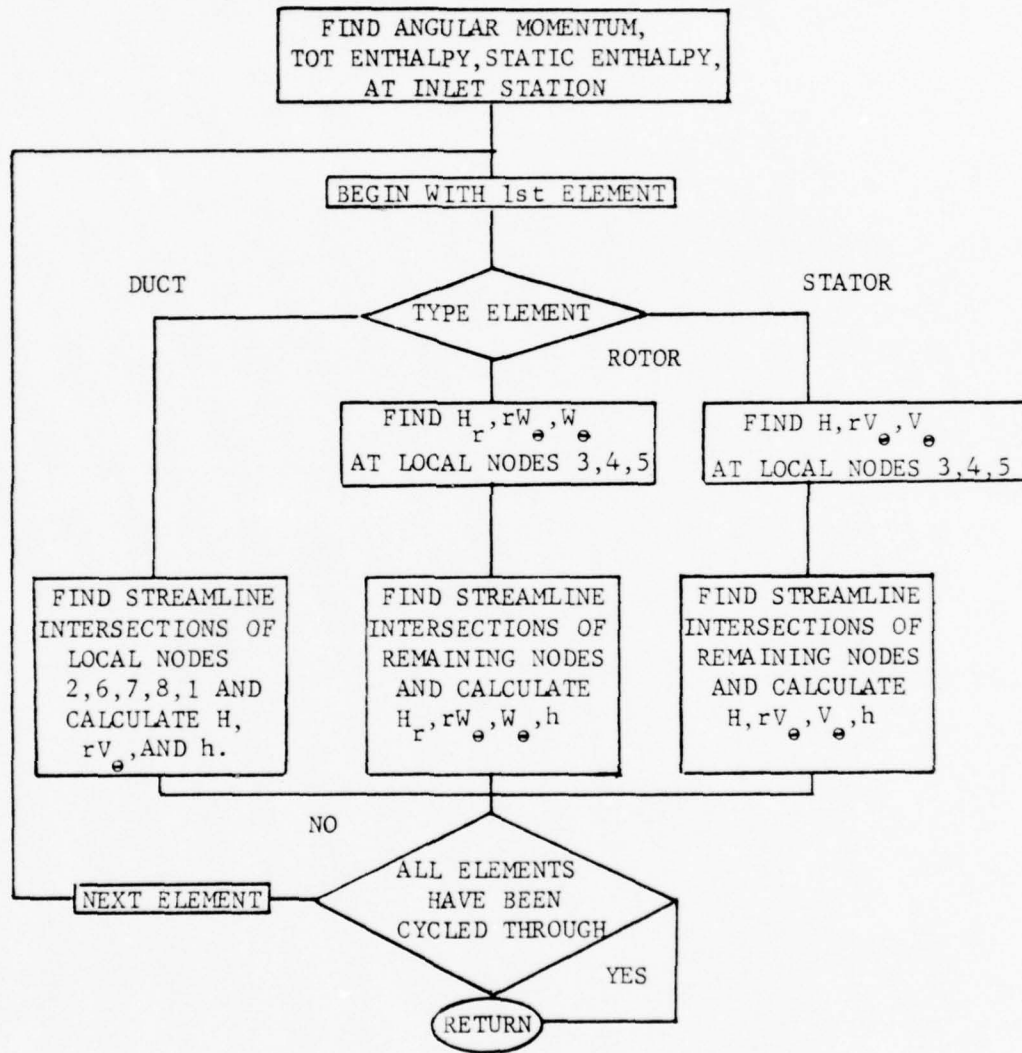


Figure 10 - SUBROUTINE SLINE

#### 4. Subroutine fcal

FCAL calculates the right hand side vector as defined by equations (II.A.31) and (II.B.21). Using the identical coordinate transformations for numerical integration as described in Section II.C, the final equation to be coded is the following,

$$f_i = \int_{-1}^1 \int_{-1}^1 \frac{N_i}{\sum N_i V_{zi}} \cdot \frac{\sum N_i V_{\theta i}}{\sum N_i R_i} \left\{ \left( L J^{-1}(z, 1) \cdot \frac{\partial N_i}{\partial \xi} + J(z, 2) \cdot \frac{\partial N_i}{\partial \eta} \right) (W_i - H_i) \right\} \det J d\xi d\eta \quad (\text{III.C.4.1})$$

where isentropic flow is assumed, and,

$W_i$  = angular momentum

(III.C.4.2)

$H_i$  = total enthalpy

The argument list is defined below. In addition, only those variables in the list which have not been defined previously are described.

SUBROUTINE FCAL(F, W, H, ZA, EA, UVEL, RC, ZC, WRL, TVEL, NFS, NODE, NN, NE, NNFSP, TWEL, NPE)

F = Right hand side vector,  $f(r, z)$

W = vector of gaussian quadrature coefficients

ZA = Vector of  $\xi_i$  gaussian quadrature points

EA = Vector of  $\eta_i$  gaussian quadrature points

NFS = Vector containing nodes where the right hand side

is to be specified

NN = number of nodes

NE = number of elements

NNFSP = Number of nodes where the right hand side is specified

Fig 11 depicts the basic flowchart for the subroutine. To initialize the procedure, one begins with the first node (upper right hand corner) of the first element. A switch is then applied which determines if the right hand side is to be calculated at the node or if a stream function value has been specified. This information is transferred from the main program through the argument list. Once the node is allowed through the switch, then the integration process is started at the first integration point. As in Section III.A.2, the flowchart depicts a three-point Gauss Quadrature scheme. After the integration has been completed, a switch determines if all the local nodes in the element have been cycled through and if so, then the assembly of the elemental vector,  $F^e$ , is performed to build the system right hand side vector,  $F$ . Finally, the subroutine determines if all the elements have been examined in order to signal completion of the right hand side vector. At this point, the vector,  $F(r,z)$ , is returned to the main program for problem solution.

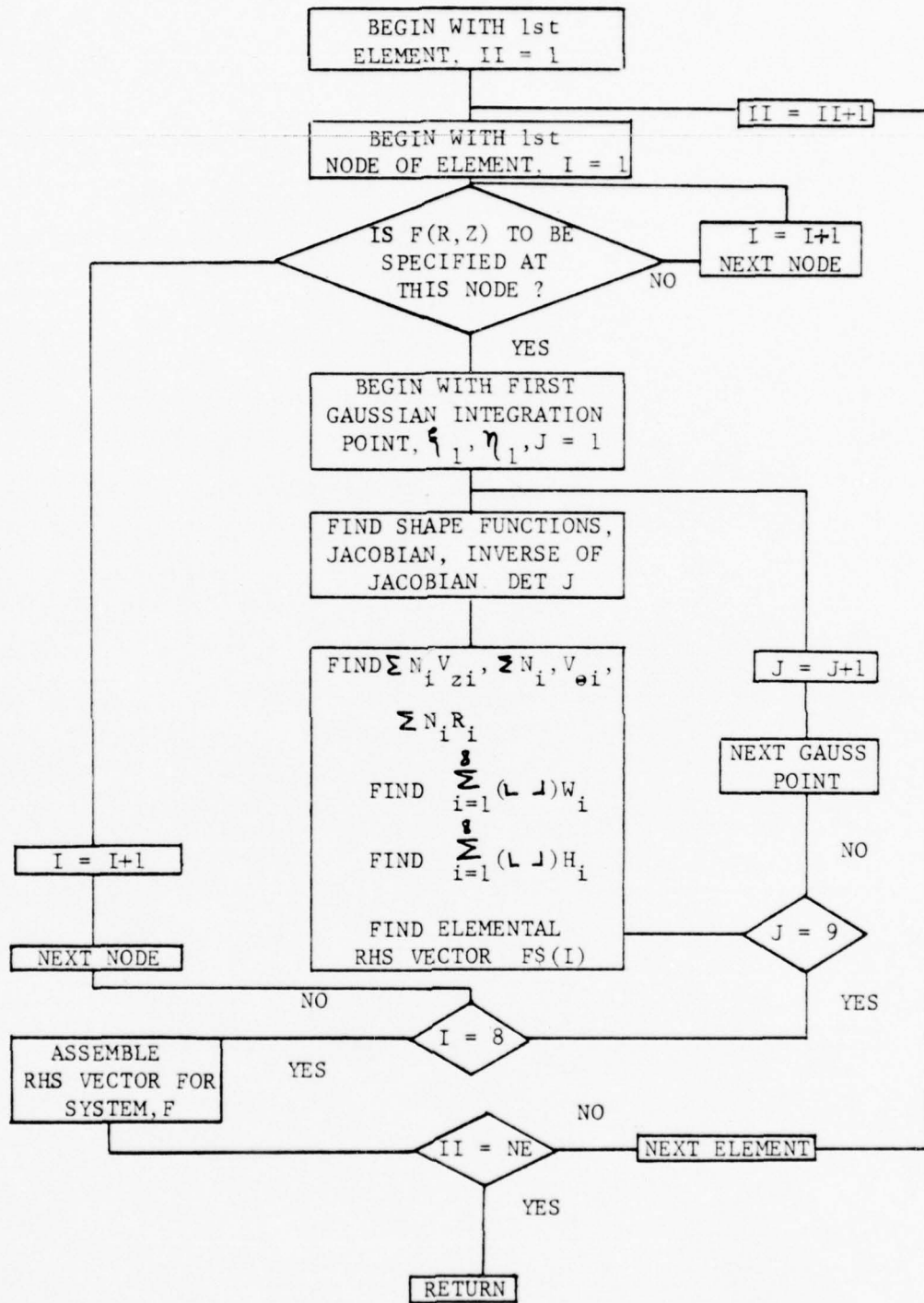


Figure 11 - SUBROUTINE FCAL

5. Subroutine vel

This subroutine calculates axial and radial velocities and also densities at each of the nodes from a known stream function distribution. As noted previously in Section II.C.2, both velocity and density profiles are updated after obtaining the latest value of nodal stream function.

The velocity calculation proceeds from the stream function equations,

$$V_z = \frac{1}{\rho r b} \frac{\partial \psi}{\partial r} \quad (\text{III.C.5.1})$$

$$V_r = -\frac{1}{\rho r b} \frac{\partial \psi}{\partial z} \quad (\text{III.C.5.2})$$

where 'b' is the tangential blockage factor. Since  $r$ ,  $\rho$ , and  $b$  are of the following form,

$$\begin{aligned} r &= \sum_{i=1}^8 r_i N_i \\ \rho &= \sum_{i=1}^8 \rho_i N_i \\ \psi &= \sum_{i=1}^8 N_i \psi_i \end{aligned} \quad (\text{III.C.5.3})$$

then the equation for the axial velocity,  $V_z$ , becomes,

$$V_z = \frac{1}{b \sum_{i=1}^8 \rho_i N_i \sum_{i=1}^8 N_i r_i} \left[ \sum_{i=1}^8 \frac{\partial N_i}{\partial r} \psi_i \right] \quad (\text{III.C.5.4})$$

Again, since the shape function,  $N_i(\eta, \gamma)$ , is not an

implicit function of 'r' and 'z', one must use equation (II.C.1.5) to obtain the proper derivatives for computation of equation (III.C.5.4). For example, from equation (III.C.5),

$$\sum_{i=1}^8 \frac{\partial N_i}{\partial r} = \sum_{i=1}^8 \left[ J^{-1}(1,1) \frac{\partial N_i}{\partial \xi} + J^{-1}(1,2) \frac{\partial N_i}{\partial \eta} \right] \quad (\text{III.C.5.5})$$

At this point, with equation (III.C.5.5) substituted into equation (III.C.5.4), one has the complete expression for the axial velocity as functions of  $\xi, \eta$ . One proceeds similarly for expressing the radial velocity,  $V$ , in terms of  $\xi$  and  $\eta$ .

In order to calculate the nodal density, one uses the following density relation for flows in the stator and duct regions.

$$\frac{p}{p_t} = \left( 1 - \frac{\gamma-1}{2a_0} V^2 \right)^{\frac{1}{\gamma-1}} \quad (\text{III.C.5.6})$$

where  $p_t$  is the stagnation density.

Since,

$$V^2 = (V_z^2 + V_r^2)(1 + \tan^2 \alpha) \quad (\text{III.C.5.7})$$

then,

$$\frac{p}{p_t} = \left[ 1 - \frac{\gamma-1}{2a_0} \left( \frac{1}{\rho r b} \right)^2 (\psi_r^2 + \psi_z^2) (1 + \tan^2 \alpha) \right]^{\frac{1}{\gamma-1}} \quad (\text{III.C.5.8})$$

Since the density appears on both sides of the equation, the new nodal density is obtained iteratively at the node.

For the relative flows in the rotor, the following relation for static density is used [Ref.14].

$$\frac{p}{p_t} = \left[ 1 - (\gamma-1) \frac{\omega R V_0}{a_0^2} - \frac{(\gamma-1)}{2} \frac{W^2 - \omega^2 R^2}{a_0^2} \right]^{\frac{1}{\gamma-1}} \quad (\text{III.C.5.9})$$

Again, the solution of the nodal density is obtained in an iterative fashion.

In the following argument list, only those variables not defined in the previous subroutine descriptions are noted.

SUBROUTINE VEL(NE, NN, RC, NODE, G, RG, TT, RHOT, RHON, ZC, PSI, RHO, B, UINLET, UVEL, VVEL, RHOSTA, NPE, ALP)

G = Ratio of specific heats

RG = Gas constant

RHOT = Total density at the inlet

RHON = work vector which contains the new nodal density distribution

RHO = Nodal static density vector

B = nodal blockage factor vector

RHOSTA = Static density at the inlet station

The basic flowchart for SUBROUTINE VEL is shown in Fig 12. Beginning with the first node of the first element, the Jacobian matrix (equation (II.C.1.4)) and its inverse

are found. At this point the partial derivatives with respect to 'r' and 'z' of the shape functions are found as noted in equation (III.C.5.5). A switch then allows those nodes not at the inlet station to pass and calculates the new density and velocities at the nodes. For those nodes at the inlet, the velocities and static densities are retained at the given inlet conditions. This is done to maintain boundary condition integrity for the solution. After cycling through all elements, the subroutine returns the new nodal velocity and density distributions to the main program.

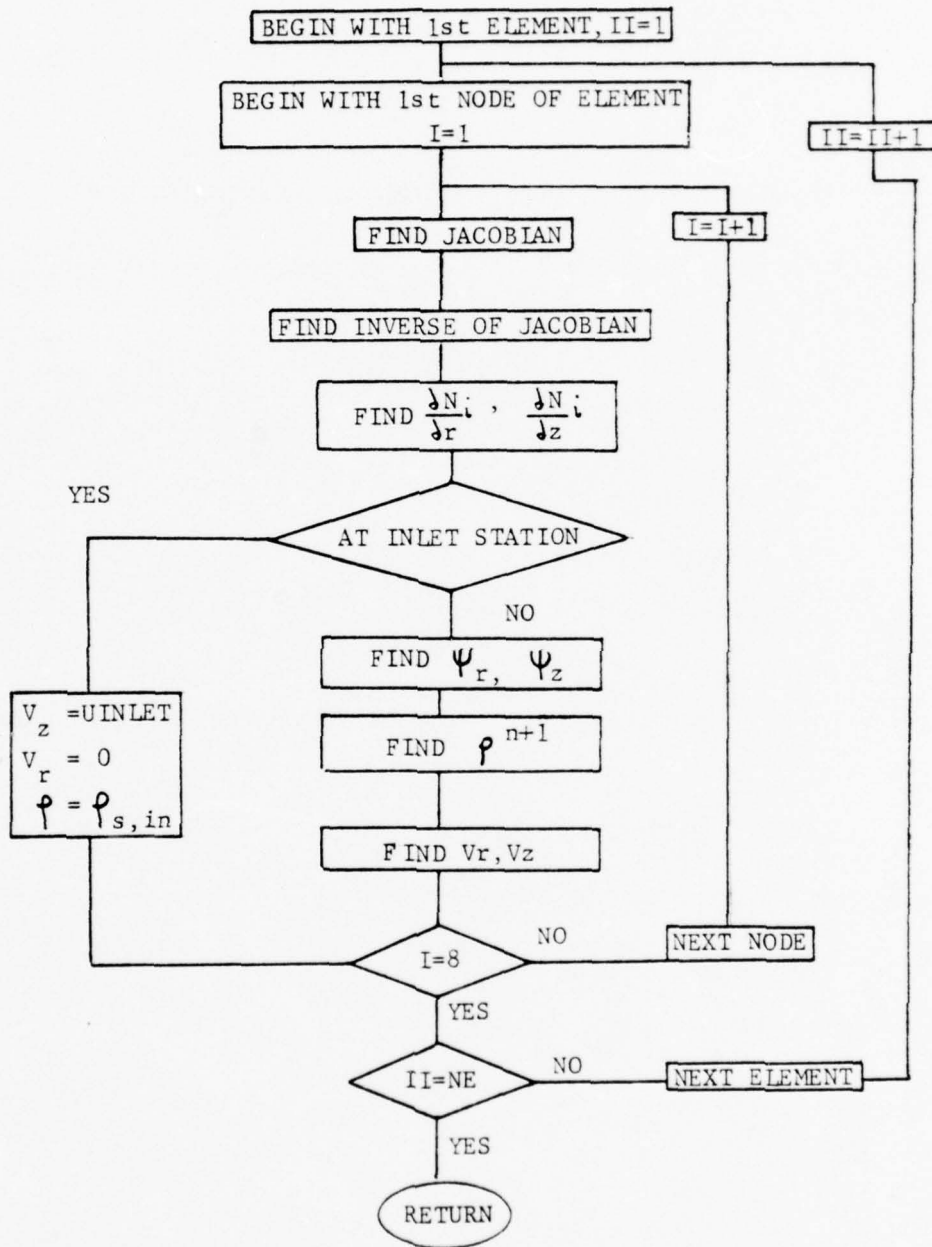


Figure 12 - SUBROUTINE VEL

## 6. Subroutine mplot

This subroutine utilizes the Calcomp plotter to depict the mesh topology of the machine under observation.

```
SUBROUTINE MPLOTT(RC,ZC,NODE,NN,NE)
```

This completes the description of the main program and associated subroutines. In the next section, a test case is carried through from data input to final results.

#### IV. TEST CASES AND RESULTS

The program was tested by using published performance data [Ref.12] of the NASA Task-1 stage transonic compressor. The compressor was discretized into twenty-eight elements and 107 nodes with 15 axial calculation stations (Fig 6). The speed was 0.5 design speed with a mass flow of 107.6 lbm/sec. In addition, uniform flow was assumed both at the inlet and outlet stations. Turning angles for the rotor and stator were pre calculated assuming uniform conditions at the rotor inlet and using NASA SP-36 blade correlation data [Ref.13]. These absolute and relative flow angles were assumed constant throughout the iterative procedure as they were an integral part of the input data. The Appendix contains a listing of the input data and output results for the NASA Task-1 transonic compressor with test conditions noted. To compare the accuracy of the predicted flow with actual laboratory observations, computed axial velocity profiles at the rotor inlet, rotor outlet, stator inlet, and stator outlet were compared with experimental results. In addition numerical results from Ref.7 were also compared.

Fig 13-16 show the computer predictions plotted with the experimental values and the numerical solutions obtained by Hirsch and Warzee. The profiles shown were obtained after ten iterations and using a relaxation factor of 0.2. The figures show that the best overall agreement with experimental data occurred in the stator inlet and outlet. In this region the worst error was 17% which occurred at the stator tip inlet. The average error throughout the stator region with respect to experimental data was 6.6%.

The rotor hub and tip outlet area exhibited instabilities in density convergence using equation III.C.5.9. Specifically, the density solution converged to within 8% at the rotor outlet tip and hub. It was found that by not allowing the nodal density at these nodes to go below a critical value of 0.06 lbm/cu ft, the solution for the stream function converged. By allowing the nodal densities at the rotor outlet tip and hub to go below this critical value, the computed velocities at these nodes became increasingly large and the argument within the brackets of equation III.C.5.9 became less than one. This prevented continuation of the iterations for the stream function solution. In addition, the rotor tip outlet exhibited more instability than the rotor hub outlet. The static density at the rotor hub outlet oscillated about a value of 0.062 lbm/cu ft while the rotor tip outlet was constantly driven to the critical value of 0.06 lbm/cu ft. One method attempted to alleviate this problem was the following. Since a half-interval iteration routine was used, one trial run involved reversing the direction of consecutive guesses when the density iteration did not converge. It was found however, that after three to four iterations of the system of equations, the static densities at the rotor outlet tip and hub were again driven to smaller and smaller values which led to instability once more. The nodal densities converged at all interior points of the rotor edge and mid-blade regions and also at all the rotor inlet nodes. By including all rotor nodes, the average error with respect to experimental data was 27.5%.

Fig 17 shows a plot of convergence criteria,  $\epsilon$ , versus the number of iterations for a relaxation factor of 0.2. The stability of convergence is shown to initially decrease and then after the third iteration oscillates about an approximate value of 28%. It is important to note that this curve represents the maximum value of  $\epsilon$  as shown in equation

(II.C.2.5). In addition, the curve in actuality represents the oscillation of nodal stream function values in the rotor/stator regions since in fact this is where the non-linearity is the greatest.

## V. CONCLUSIONS AND RECOMMENDATIONS FOR FURTHER STUDY

Agreement with both experimental data and numerical solution of Ref.7 was best in the stator region to within 8%. Predicted axial velocity profiles in the rotor inlet area were within 26.2% of experimental results. The instabilities with respect to static density solutions are prevalent. One of the reasons for this numerical disagreement with Hirsch and Warzee is the isentropic assumption imposed by the present program. Recommendations for further study on the project include the addition of entropy variations in the rotor and stator blade regions. This would necessitate the use of blade correlation data [Ref.13] for loss predictions and involve additional input data plus program additions to Subroutine's SLINE and FCAL.

RADIUS (IN)

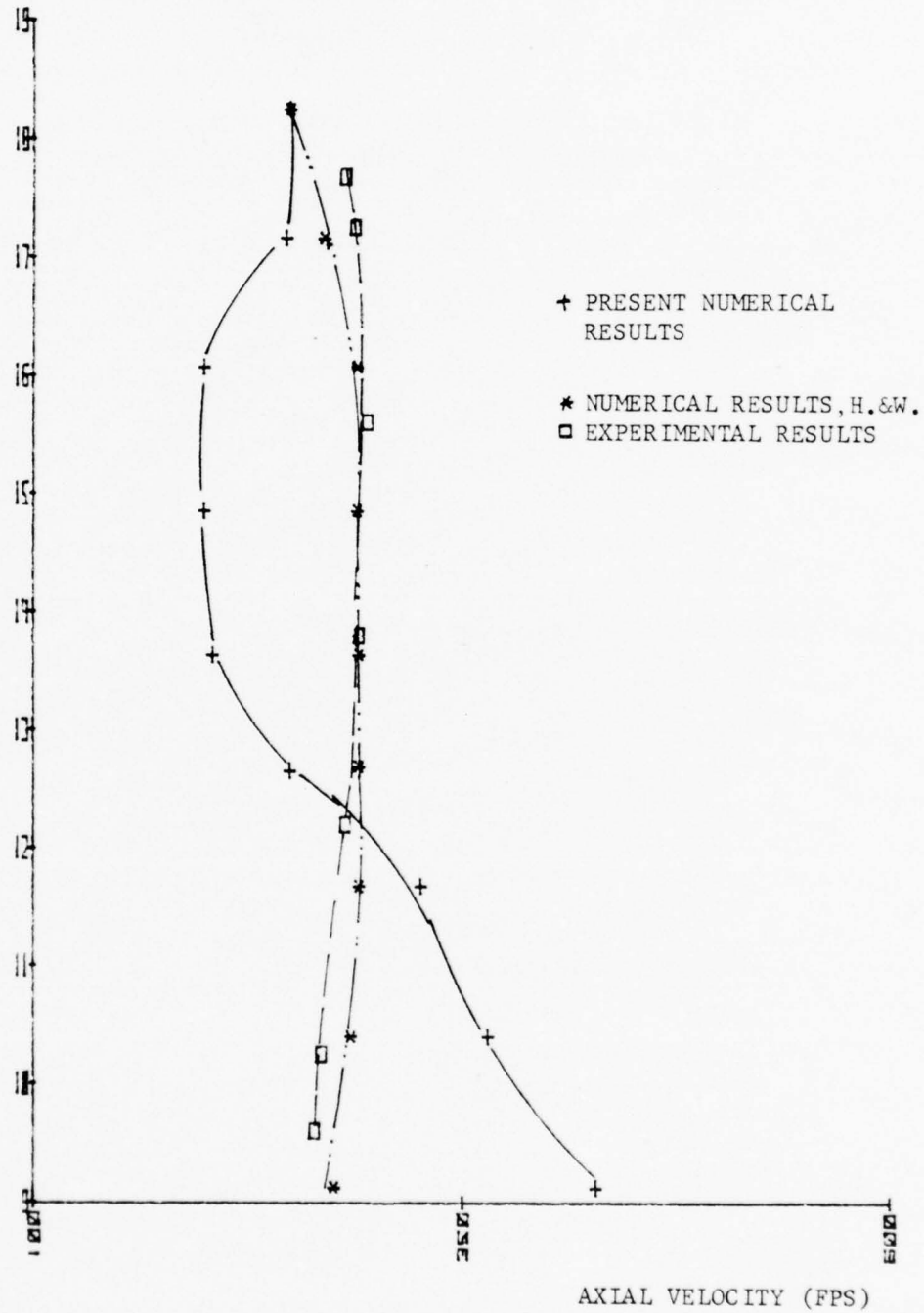


Figure 13 - AXIAL PROFILE AT ROTOR INLET

RADIUS (IN)

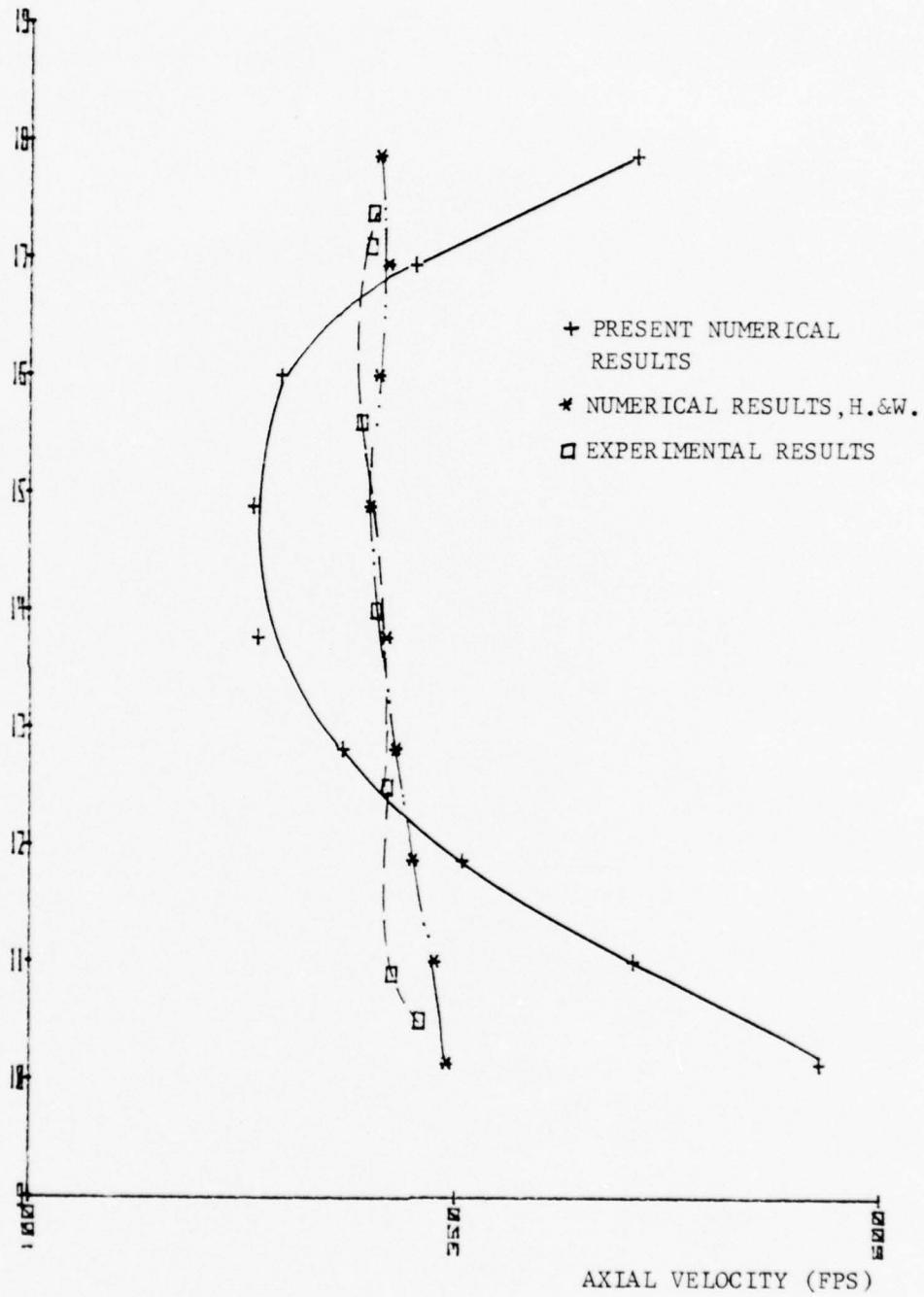


Figure 14 - AXIAL PROFILE AT ROTOR OUTLET

RADIUS (IN)

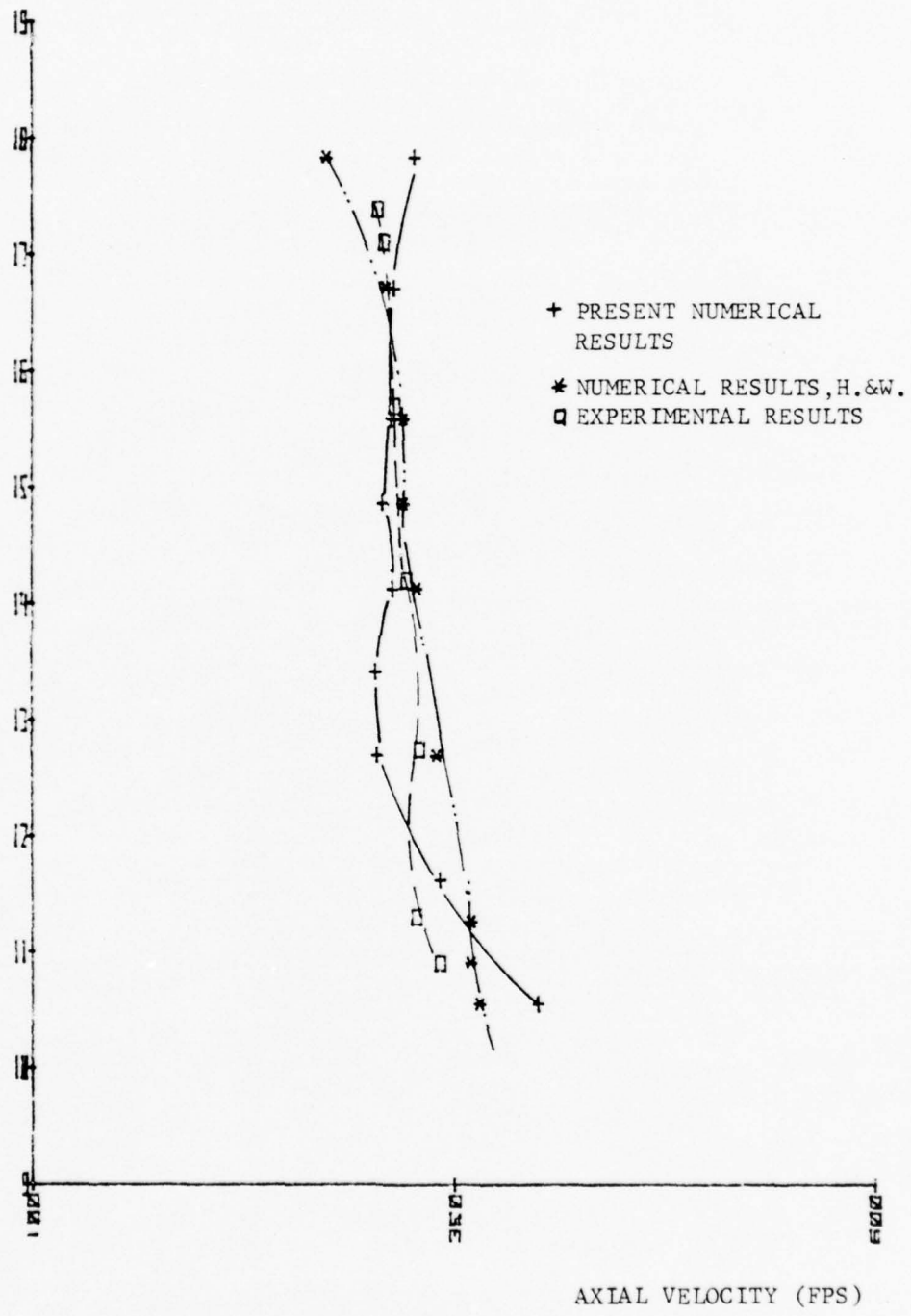


Figure 15 - AXIAL PROFILE AT STATOR INLET

RADIUS (IN)

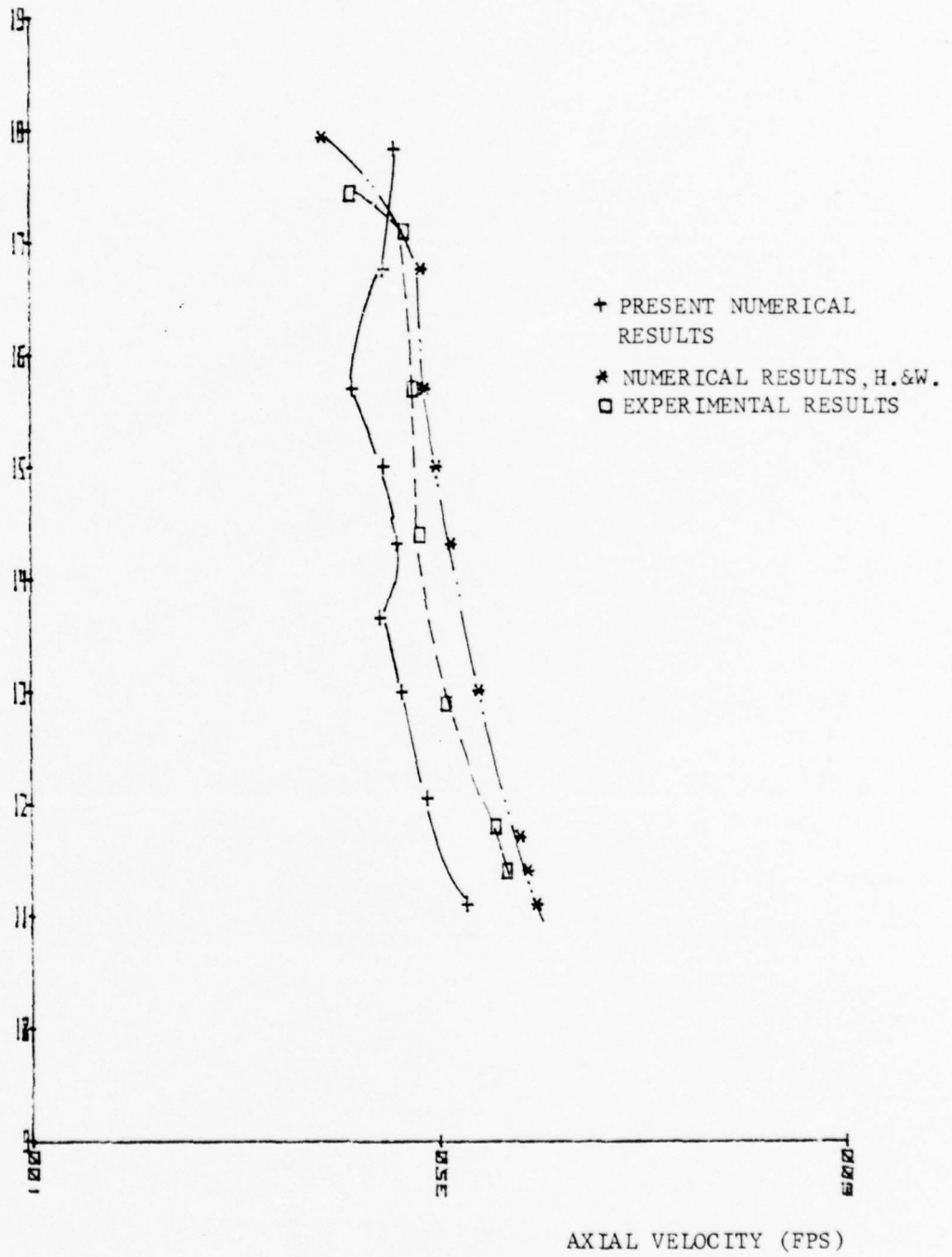


Figure 16 - AXIAL PROFILE AT STATOR OUTLET

EPSILON

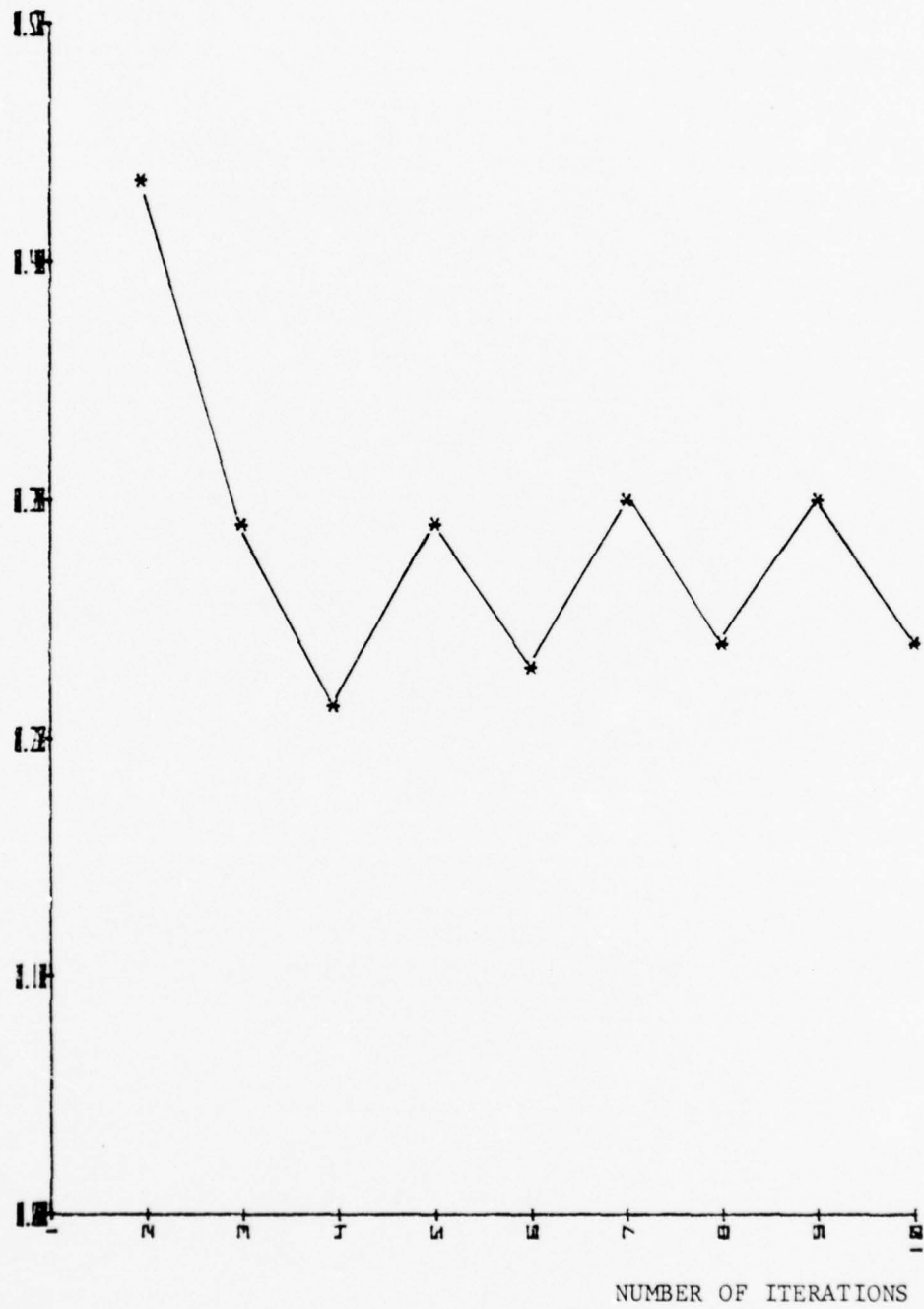


Figure 17 - EPSILON VS. ITERATIONS





```

160      EM$(I,J) = 0.00
        CONTINUE
        DO 165 I = 1,NE
          NTE(I) = 0
          RHOE(I) = 0.00
          R(I) = 0.00
          DO 165 J = 1,8
            NODE(I,J) = 0
          CONTINUE
          READ NODE NUMBERS,NODAL COORDINATES (IN INCHES), AND NODAL
          BLOCKAGE FACTOR. INLET STATION ZC(I) MUST BE = 0.00.
          LAST NODAL ZC(NN) MUST BE AT THE OUTLET STATION.
          DO 170 J = 1,NN
            READ(NR,1000) I,ZC(I),RC(I),B(I)
            FORMAT(110,3F10.0)
          CONTINUE
          READ IN SYSTEM TOPOLOGY,I.E.,ELEMENT NO. AND LOCAL NODE NUMBERS.
          STARTING AT UPPER RIGHT HAND CORNER AND TRAVERSING IN A CCW
          FASHION AROUND THE QUADRILATERAL.
          DO 180 L = 1,NE
            READ(NR,1010) J,NODE(J,1),NODE(J,2),NODE(J,3),NODE(J,4)
            1,NODE(J,5),NODE(J,6),NODE(J,7),NODE(J,8)
            FORMAT(9I5)
          CONTINUE
          READ IN TYPE OF ELEMENT: NTE(I)=1(DUCT),NTE(I)=2(ROTOR)
          NTE(I)=3(STATOR)
          DO 185 I = 1,NE
            READ(NR,1011) J,NTE(J)
            FORMAT(2I10)
          CONTINUE
          READ IN STATOR/ROTOR NODAL ABS FLOW ANGLES
          REMEMBER THAT THIS ASSUMES UNIFORM FLOW CONDITIONS AT
          ROTOR INLET.
          DO 186 I = 1,NN
            READ(NR,1012)WORD,J,ANGLE
            FORMAT(6X,A4,I10,F10.0)
            IF(WORD.EQ.STOP)GOTO1014
            ALP(J) = ANGLE
          CONTINUE
          READ IN ROTOR NODAL REL FLOW ANGLES.

```

```

STR00970
STR00980
STR00990
STR01000
STR01010
STR01020
STR01030
STR01040
STR01050
STR01060
STR01070
STR01080
STR01090
STR01100
STR01110
STR01120
STR01130
STR01140
STR01150
STR01160
STR01170
STR01180
STR01190
STR01200
STR01210
STR01220
STR01230
STR01240
STR01250
STR01260
STR01270
STR01280
STR01290
STR01300
STR01310
STR01320
STR01330
STR01340
STR01350
STR01360
STR01370
STR01380
STR01390
STR01400
STR01410
STR01420
STR01430
STR01440

```





```

C
C
C
C
C
1030
200
201
C
C
C
210
C
C
220
C
C
C
C
C
221
1038
1040
1045
1050
1060
1062

```

RECOUNT NUMBER OF NODES WITH SPECIFIED PSI BY INCLUDING THE INLET AND OUTLET NODES.

```

NNSPSI = NNSPSI + NNODEO
READ NODES WHERE F(R,Z) IS SPECIFIED
DO 200 I = 1, NN
READ(NREAD,1030) WORD,NFSP
FORMAT(6X,A4,I10)
IF(WORD.EQ.'STOP')GOTO201
NFS(I) = NFSP
CONTINUE
NNFSP = I-1

```

NFIS IS A LIST OF THE INDICES OF THE KNOWN F(R,Z)

```

DO 210 I = 1,NNFSP
NFIS(I) = NFS(I)
CONTINUE

```

NPSI IS A LIST OF THE INDICES IF THE KNOWN PSI

```

DO 220 I = 1,NNSPSI
NPSI(I) = NPSIS(I)
CONTINUE

```

NTOTF IS THE TOTAL NUMBER OF KNOWN F(R,Z)

```

NTOTF = NNFSP

```

NTOTP IS THE TOTAL NUMBER OF KNOWN PSI

```

NTOTP = NNSPSI
PRINT ALL INPUT DATA

```

GO TO 1101

```

WRITE(NWRITE,1038)TITLE
FORMAT(1,1,20X,10A4)
WRITE(NWRITE,1040)NN,NE
FORMAT(1,1,4X,NO. OF NODES = ,I3,/,5X,
1,NO. OF ELEMENTS = ,I2)
WRITE(NWRITE,1045)
FCRMAT(1,1,20X,SUMMARY OF NODAL COORDINATES,1)
WRITE(NWRITE,1050)
FCRMAT(1,1,NODE,5X,Z(I),11X,R(I),11X,B(I),
1,7X,ABS FLOW ANG,3X,REL FLOW ANG,1)
WRITE(NWRITE,1060)(I,ZC(I),RC(I),B(I),ALP(I),BE(I),I=1,NN)
FORMAT(1,1,13,2X,E13.6,2X,E13.6,2X,E13.6)
WRITE(NWRITE,1062)
FORMAT(1,1,20X,SYSTEM TOPOLOGY,/,2X,ELEMENT,1)
110X,NODES,40X,TYPE OF ELEMENT,1)
WRITE(NWRITE,1063)(I,NODE(I,1),NODE(I,2),NODE(I,3),NODE(I,4)

```











```

4321 DO 4321 I = 1, NN
      UVEL(I) = UVEL(I)/12.00
      VVEL(I) = VVEL(I)/12.00
      CONTINUE
2345 DO 2345 I = 1, NN
      UVEL(I) = UVEL(I)*12.00
      VVEL(I) = VVEL(I)*12.00
      CONTINUE
      COMPARE 'NEW STREAM FUNCTION' DISTRIBUTION WITH 'OLD
      STREAM FUNCTION DISTRIBUTION.'
      X = 0.00
      DO 430 I = 1, NN
        IF(PSI(I).EQ.0.00)GOTO421
        EPS = DABS((PSI(I) - PSI(I))/PSI(I))
        GOTO422
      EPS = DABS(PSI(I) - PSI(I))
      IF (X.GT.EPS)GOTO430
      X = EPS
      CONTINUE
      ASK IF STREAM FUNCTION CONVERGENCE CRITERION BEEN SATISFIED?
      IF IT HAS.....WRITE RESULTS
      IF NOT.....ITERATE ONCE MORE.
      KK = KK + 1
      IF(X.LE.1.D-01 )GOTO450
      WRITE (NWRITE,1400)KK,X
      FORMAT(10,10,LARGEST EPS FOR ITERATION ',I2,' IS ',D19.12)
      IF (KK.LT.2)GOTO1500
      WRITE(NWRITE,1600)KK,X
      FORMAT(10,10,PROGRAM TERMINATED ON ITERATION NO.',I3,/,
      1, RESULTS WHICH FOLLOW ARE FOR CONVERGENCE EPSILON = ',D19.12)
      GOTO1104
      WRITE(NWRITE,1102)KK
      FORMAT(10,10,ITERATION NO.',I3,/, COMPLETE',/, STREAM FUNCTION CON
      1, VERGENCE NOT YET SATISFIED.',/, NEXT ITERATION IS IN PROGRESS.)
      NEXT ITERATION
      ZEROIZE STIFFNESS MATRIX AND RIGHT HAND SIDE VECTOR TO
      PREPARE FOR NEXT ITERATION.
      DO 460 I = 1, NN
      F(I) = 0.00
      DO 460 J = 1, NN

```

```

STR05280
STR05290
STR05300
STR05310
STR05320
STR05330
STR05340
STR05350
STR05360
STR05370
STR05380
STR05390
STR05400
STR05410
STR05420
STR05430
STR05440
STR05450
STR05460
STR05470
STR05480
STR05490
STR05500
STR05510
STR05520
STR05530
STR05540
STR05550
STR05560
STR05570
STR05580
STR05590
STR05600
STR05610
STR05620
STR05630
STR05640
STR05650
STR05660
STR05670
STR05680
STR05690
STR05700
STR05710
STR05720
STR05730
STR05740
STR05750

```



```

DIMENSION TVEL(107)
DIMENSION H(107),TWEL(107),F$(8),NFS(107),NODE(28,8),N(8),L1(2)
DIMENSION M1(2),NTE(40)
C C C C C C C
THIS SUBROUTINE CALCULATES THE RIGHT-HAND SIDE VECTOR
F(R,Z) FROM KNOWN RADIAL DISTRIBUTIONS OF WHIRL, ENTHALPY
,ROTHALPY, AND ENTROPY.
ZEROIZE OUT F$( ) .
DO 50 I = 1,8
F$(I) = 0.00
CONTINUE
50 C C C
CYCLE FOR EACH ELEMENT.
DO 100 II = 1,NE
RC$(1) = RC(NODE(II,1))
RC$(2) = RC(NODE(II,2))
RC$(3) = RC(NODE(II,3))
RC$(4) = RC(NODE(II,4))
RC$(5) = RC(NODE(II,5))
RC$(6) = RC(NODE(II,6))
RC$(7) = RC(NODE(II,7))
RC$(8) = RC(NODE(II,8))
ZC$(1) = ZC(NODE(II,1))
ZC$(2) = ZC(NODE(II,2))
ZC$(3) = ZC(NODE(II,3))
ZC$(4) = ZC(NODE(II,4))
ZC$(5) = ZC(NODE(II,5))
ZC$(6) = ZC(NODE(II,6))
ZC$(7) = ZC(NODE(II,7))
ZC$(8) = ZC(NODE(II,8))
C C C
CYCLE FOR EACH LOCAL NODE.
DO 200 I = 1,8
CHECK TO SEE IF PSI HAS BEEN SPECIFIED AT THE NODE. . . .
IF SO . . . . DO NOT CALCULATE A VALUE OF F(R,Z) FOR THE
NODE TO AVOID OVER SPECIFICATION AND CYCLE FOR THE NEXT
NODE.
DO 210 L = 1,NNFSP
LTEST = NODE(II,I) - NFS(L)
IF(LTEST.EQ.0)GOTO220
CONTINUE
GOTO200
210 C C C C C C

```

```

STR06240
STR06250
STR06260
STR06270
STR06280
STR06290
STR06300
STR06310
STR06320
STR06330
STR06340
STR06350
STR06360
STR06370
STR06380
STR06390
STR06400
STR06410
STR06420
STR06430
STR06440
STR06450
STR06460
STR06470
STR06480
STR06490
STR06500
STR06510
STR06520
STR06530
STR06540
STR06550
STR06560
STR06570
STR06580
STR06590
STR06600
STR06610
STR06620
STR06630
STR06640
STR06650
STR06660
STR06670
STR06680
STR06690
STR06700
STR06710

```



STR07200  
 STR07210  
 STR07220  
 STR07230  
 STR07240  
 STR07250  
 STR07260  
 STR07270  
 STR07280  
 STR07290  
 STR07300  
 STR07310  
 STR07320  
 STR07330  
 STR07340  
 STR07350  
 STR07360  
 STR07370  
 STR07380  
 STR07390  
 STR07400  
 STR07410  
 STR07420  
 STR07430  
 STR07440  
 STR07450  
 STR07460  
 STR07470  
 STR07480  
 STR07490  
 STR07500  
 STR07510  
 STR07520  
 STR07530  
 STR07540  
 STR07550  
 STR07560  
 STR07570  
 STR07580  
 STR07590  
 STR07600  
 STR07610  
 STR07620  
 STR07630  
 STR07640  
 STR07650  
 STR07660  
 STR07670

```

130 CONTINUE
C
C
C
131 FIND F$(NODE(II,1))
XX = SUMH + (SUMV/SUMR)*SUMW
XX = (SF(I)/SUMU)*XX*DETJ
F$(I) = F$(I) + XX*W(J)
CONTINUE
200 CONTINUE
C
C
C
ASSEMBLE RIGHT HAND SIDE VECTOR.
N(1) = NODE(II,1)
N(2) = NODE(II,2)
N(3) = NODE(II,3)
N(4) = NODE(II,4)
N(5) = NODE(II,5)
N(6) = NODE(II,6)
N(7) = NODE(II,7)
N(8) = NODE(II,8)
DO 400 I$ = 1,8
I = N(I$)
F(I) = F(I) + F$(I$)
CONTINUE
400
C
C
C
500 DO 500 I = 1,8
F$(I) = 0.00
CONTINUE
C
C
C
100 RETURN
DEBUG SUBCHK
END
SUBROUTINE JACOB(E1,Z1,D,E,RC$,ZC$,RJAC)
IMPLICIT REAL*8(A-H,P-Z)
NEXT ELEMENT.
THIS SUBROUTINE CALCULATES THE JACOBIAN MATRIX FOR SUBSE-
QUENT NUMERICAL INTEGRATIONS BY GAUSSIAN QUADRATURE.
DIMENSION RJAC(2,2),D(8),E(8),RC$(8),ZC$(8)
RJAC(1,1) = 0.00
RJAC(1,2) = 0.00
RJAC(2,1) = 0.00
RJAC(2,2) = 0.00
D(1) = (E1 + 2.00*Z1 + 2.00*Z1*E1 + E1*E1)/4.00

```

```

STR07680
STR07690
STR07700
STR07710
STR07720
STR07730
STR07740
STR07750
STR07760
STR07770
STR07780
STR07790
STR07800
STR07810
STR07820
STR07830
STR07840
STR07850
STR07860
STR07870
STR07880
STR07890
STR07900
STR07910
STR07920
STR07930
STR07940
STR07950
STR07960
STR07970
STR07980
STR07990
STR08000
STR08010
STR08020
STR08030
STR08040
STR08050
STR08060
STR08070
STR08080
STR08090
STR08100
STR08110
STR08120
STR08130
STR08140
STR08150

D(2) = -(Z1 + Z1*E1)
D(3) = (-E1 + 2.00*Z1 + 2.00*Z1*E1 - E1*E1)/4.00
D(4) = (-1.00 + E1*E1)/2.00
D(5) = (E1 + 2.00*Z1 - 2.00*Z1*E1 - E1*E1)/4.00
D(6) = (-Z1 + Z1*E1)
D(7) = (-E1 + 2.00*Z1 - 2.00*Z1*E1 + E1*E1)/4.00
D(8) = (1.00 - E1*E1)/2.00
E(1) = (Z1 + 2.00*E1 + Z1*Z1 + 2.00*Z1*E1)/4.00
E(2) = (1.00 - Z1*Z1)/2.00
E(3) = (-Z1 + 2.00*E1 + Z1*Z1 - 2.00*Z1*E1)/4.00
E(4) = (-E1 + E1*Z1)
E(5) = (Z1 + 2.00*E1 - Z1*Z1 - 2.00*Z1*E1)/4.00
E(6) = (-1.00 + Z1*Z1)/2.00
E(7) = (-Z1 + 2.00*E1 - Z1*Z1 + 2.00*Z1*E1)/4.00
E(8) = -(E1 + Z1*E1)
DO 100 I = 1,8
RJAC(1,1) = RJAC(1,1) + D(I)*ZC$(I)
RJAC(1,2) = RJAC(1,2) + D(I)*RC$(I)
RJAC(2,1) = RJAC(2,1) + E(I)*ZC$(I)
RJAC(2,2) = RJAC(2,2) + E(I)*RC$(I)
CONTINUE
RETURN
DEBUG SUBCHK
END
SUBROUTINE VEL(NN,RC,NODE,G,RG,TT,RHOT,RHON,ZC,PSI,RHO,B,UIINLET
1,UVEL,VVEL,RHOSTA,ALP,BE,H,WC)
C
C THIS SUBROUTINE CALCULATES U AND V VELOCITIES AND A NEW
C NODAL DENSITY FROM A KNOWN PSI DISTRIBUTION AT EACH OF
C THE NODES IN THE SYSTEM. IN ADDITION, THE CALL STATEMENTS
C TRANSFERS THE NUMBER OF ELEMENTS, NODAL COORDINATES, LOCAL
C NODE NUMBERS, RATIO OF SPECIFIC HEATS, GAS CONSTANT, TOTAL
C TEMPERATURE, TOTAL DENSITY, THE LATEST CALCULATED NODAL
C STREAM FUNCTION, DENSITY DISTRIBUTION, NODAL BLOCKAGE FAC-
C TOR, AND INLET VELOCITY CONDITIONS.
C
C IMPLICIT REAL*8(A-H,P-Z)
C DIMENSION RJAC(2,2),PSI(107),D(8),E(8),UVEL(107),VVEL(107)
C DIMENSION RC$(8),ZC$(8),RC(107),RHO(107),EI(8),ZI(8)
C DIMENSION DR(8),DZ(8),B(107),RHON(107),ALP(107),BE(107)
C DIMENSION NODE(28,8),LI(2)
C DIMENSION MI(2)
C DATA ZI/1.00,0.00,-1.00,-1.00,0.00,1.00,1.00,0.00/
C DATA EI/1.00,1.00,1.00,-1.00,-1.00,-1.00,-1.00,0.00/
C DO 100 I = 1,NE
C RC$(1) = RC(NODE(I,1))
C RC$(2) = RC(NODE(I,2))
C RC$(3) = RC(NODE(I,3))
C RC$(4) = RC(NODE(I,4))

```

100



```

301 IDEN = IDEN + 1
IF(NODE(II,I).LT.43)GOTO300
IF(NODE(II,I).GT.65)GOTO300
XM = (XL + XR)/2.00
R1 = RC(NODE(II,I))
B1 = B(NODE(II,I))
W1 = (PSIZ**2 + PSIR**2)/((XM*R1*B1)**2)
W1 = (W1*144.00*144.00/32.17400)/(DCOS(BETA)**2)
U1 = (WG*R1)**2/(144.00*32.17400)
A1 = (G - 1.00)*(W1 - U1)/(2.00*G*RG*TT)
A2 = DSQRT((PSIR**2 + PSIZ**2)/((XM*R1*B1)**2))*DTAN(ALPHA)
A2 = (G - 1.00)*(WG*R1)**2/(G*RG*TT)
A2 = A2*12.00/32.17400
RHON(NODE(II,I)) = RHOT*((1.00-A2-A1)**(1.00/(G-1.00)))
GOTO315
300 A1 = (G - 1.00)/(2.00*G*RG*TT)
XM = (XL + XR)/2.00
A1 = AI/((XM
*RC(NODE(II,I))*B(NODE(II,I))**2)
A1 = AI*144.00*144.00/32.17400
A1 = 1.00 - AI*(PSIZ**2 + PSIR**2*(1.00 + DTAN(ALPHA)**2))
A1 = AI**((1.00/(G - 1.00)))
RHON(NODE(II,I)) = RHOT*AI
EPS = RHON(NODE(II,I)) - XM
X4 = DABS(EPS)
IF(X4.LT.1.0D-06)GOTO250
IF(IDEN.EQ.10)GOTO250
IF(EPS.LT.0.0D0)GOTO310
XL = XM
GOTO301
XR = XM
GOTO301
IF(XM.GT.6.0D-02)GOTO255
XM = 0.6D-01
RHON(NODE(II,I)) = XM
C
C
C
FIND UVEL AND VVEL
UVEL(NODE(II,I)) = PSIR/(XM
*RC$(I)*B(NODE(II,I)))
VVEL(NODE(II,I)) = UVEL(NODE(II,I))*144.00*12.00
VVEL(NODE(II,I)) = -PSIZ/(XM
*RC$(I)*B(NODE(II,I)))
VVEL(NODE(II,I)) = VVEL(NODE(II,I))*144.00*12.00
GO TO 200
10 UVEL(NODE(II,I)) = UIMLET
VVEL(NODE(II,I)) = 0.00
RHON(NODE(II,I)) = RHOSTA
CONTINUE
200 C
C
C
C
C
C
NEXT ELEMENT
100 CONTINUE

```

```

STR08640
STR08650
STR08660
STR08670
STR08680
STR08690
STR08700
STR08710
STR08720
STR08730
STR08740
STR08750
STR08760
STR08770
STR08780
STR08790
STR08800
STR08810
STR08820
STR08830
STR08840
STR08850
STR08860
STR08870
STR08880
STR08890
STR08900
STR08910
STR08920
STR08930
STR08940
STR08950
STR08960
STR08970
STR08980
STR08990
STR09000
STR09010
STR09020
STR09030
STR09040
STR09050
STR09060
STR09070
STR09080
STR09090
STR09100
STR09110

```

STR09120  
 STR09130  
 STR09140  
 STR09150  
 STR09160  
 STR09170  
 STR09180  
 STR09190  
 STR09200  
 STR09210  
 STR09220  
 STR09230  
 STR09240  
 STR09250  
 STR09260  
 STR09270  
 STR09280  
 STR09290  
 STR09300  
 STR09310  
 STR09320  
 STR09330  
 STR09340  
 STR09350  
 STR09360  
 STR09370  
 STR09380  
 STR09390  
 STR09400  
 STR09410  
 STR09420  
 STR09430  
 STR09440  
 STR09450  
 STR09460  
 STR09470  
 STR09480  
 STR09490  
 STR09500  
 STR09510  
 STR09520  
 STR09530  
 STR09540  
 STR09550  
 STR09560  
 STR09570  
 STR09580  
 STR09590

```

DO 500 I = 1, NN
RHO(I) = RHON(I)
CONTINUE
500 C C
RETURN SUBCHK
END
SUBROUTINE SLINE(UINLET, RC, PSI, WRL, H, UVEL, VVEL, TVEL, NODE
1, INLET, NNODEI, NE, CP, TT, KK, NTE, ALP, WG, TWEL, BE, HS)
IMPLICIT REAL*8(A-H, P-Z)
DIMENSION PSI(107), SF(8), UVEL(107), VVEL(107), RC(107), WRL(107)
DIMENSION TVEL(107)
DIMENSION H(107), ALP(107), TWEL(107), BE(107), HS(107)
DIMENSION FL(8), NODE(28, 8)
DIMENSION INLET(10), NTE(40)
DATA EL/1.00, 1.00, 1.00, 0.00, -1.00, -1.00, -1.00, 0.00/
THIS SUBROUTINE CALCULATES THE THERMODYNAMIC VARIABLES
THROUGHOUT THE SYSTEM FROM GIVEN INLET CONDITIONS AT THE
DUCT. THIS IS DONE BY INITIALLY SEARCHING FOR THE
STREAMLINES AT EACH NODE AND THEN USING THE ASSUMPTION
THAT IN A DUCT REGION THE SWHRL (R#VTHETA) IS CONSTANT
IN ROTOR, HREL IS CONSTANT; AND IN STATOR, H IS CONSTANT.
FIND WHIRL AT INLET
FIND V THETA AT INLET
INSERT TOT ENTHALPY AT INLET NODES.
INSERT STATIC ENTHALPY AT INLET NODES
MM = 0
THEVEL = UINLET*DTAN(ALP(1))
DO 100 I = 1, NNODEI
WRL(INLET(I)) = RC(INLET(I))*THEVEL
H(INLET(I)) = CP*TT
HS(INLET(I)) = CP*TT - (UINLET**2)/7.20935D06
CONTINUE
100 C C C
BEGIN WITH MID NODE OF FIRST ELEMENT AND THEN CYCLE
THROUGH EACH ELEMENT.
I = II
DO 120 II = 1, NE
IF(NTE(II)).EQ.2)GOTO500
IF(NTE(II)).EQ.3)GOTO600
GOTO111
110 C C C
FIND HREL, WRL, AND TWEL AT LOC NODES 3, 4, 5 (ROTOR).

```

AD-A038 759

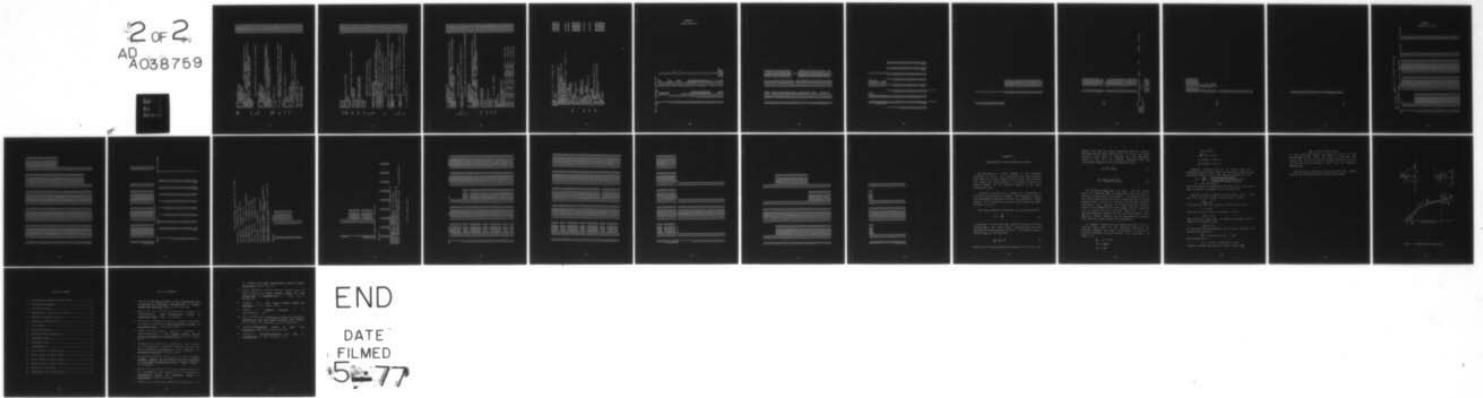
NAVAL POSTGRADUATE SCHOOL MONTEREY CALIF  
THE FINITE ELEMENT METHOD APPLIED TO FLOWS IN TURBOMACHINES.(U)  
DEC 76 V F GAVITO

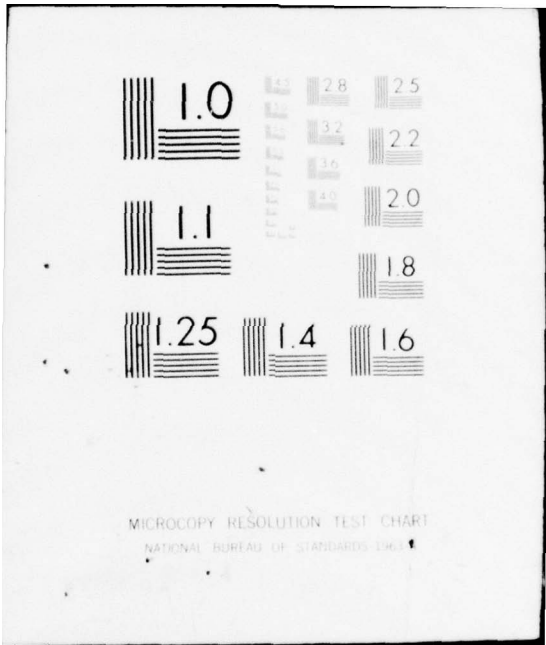
F/6 20/4

UNCLASSIFIED

NL

2 of 2  
AQ  
A038759





MICROCOPY RESOLUTION TEST CHART  
NATIONAL BUREAU OF STANDARDS-1963-A

STR09600  
 STR09610  
 STR09620  
 STR09630  
 STR09640  
 STR09650  
 STR09660  
 STR09670  
 STR09680  
 STR09690  
 STR09700  
 STR09710  
 STR09720  
 STR09730  
 STR09740  
 STR09750  
 STR09760  
 STR09770  
 STR09780  
 STR09790  
 STR09800  
 STR09810  
 STR09820  
 STR09830  
 STR09840  
 STR09850  
 STR09860  
 STR09870  
 STR09880  
 STR09890  
 STR09900  
 STR09910  
 STR09920  
 STR09930  
 STR09940  
 STR09950  
 STR09960  
 STR09970  
 STR09980  
 STR09990  
 STR10000  
 STR10010  
 STR10020  
 STR10030  
 STR10040  
 STR10050  
 STR10060  
 STR10070

```

500 DO 501 J = 3,5
502 VZ = UVEL(NODE(II,J))
  VR = VVEL(NODE(II,J))
  A = BE(NODE(II,J))
  R = RC(NODE(II,J))
  H(NODE(II,J)) = H(NODE(II,J)) - (WG*R)**2
  H(NODE(II,J)) = H(NODE(II,J))/7.209035D06 + HS(NODE(II,J))
  TWEL(NODE(II,J)) = DSQRT(VR*VR + VZ*VZ)*DTAN(A)
  WRL(NODE(II,J)) = R*(WG*R - TWEL(NODE(II,J)))
  CONTINUE
  GOT011

501 FIND H,WRL,AND TVEL AT LOC NNODES 3,4,5(STATOR).

C
C
C 600 DO 601 J = 3,5
  VZ = UVEL(NODE(II,J))
  VR = VVEL(NODE(II,J))
  A = ALP(NODE(II,J))
  R = RC(NODE(II,J))
  H(NODE(II,J)) = H(NODE(II,J))
  H(NODE(II,J)) = H(NODE(II,J)) + (VR*VR+VZ*VZ)*(1.D0+DTAN(A)**2)
  TWEL(NODE(II,J)) = DSQRT(VR*VR+VZ*VZ)*DTAN(A)
  WRL(NODE(II,J)) = R*TVEL(NODE(II,J))
  CONTINUE
  N = 2
  P = PSI(NODE(II,N))
  IT = 0
  I = II

C 130 IF(P.GE.PSI(NODE(I,5)))GOTO140
  CHECK TO SEE IF P IS WITHIN THE PRESENT ELEMENT
  CHECK NEXT ELEMENT BELOW THE PRESENT ELEMENT.

C 140 I = I + 1
  GOT0130
  IF(P.GT.PSI(NODE(I,4)))GOTO170
  EL = EI(4)
  ER = EI(5)
  E = (EL + ER)/2.D0
  CALL SHAPE(E,-1.D0,SF)
  PA = SF(3)*PSI(NODE(I,3)) + SF(4)*PSI(NODE(I,4))
  I + SF(5)*PSI(NODE(I,5))
  CHECK FOR STREAMLINE CONVERGENCE

C 150 EPS = DABS(PA - P)
  IF(EPS.LT.1.D-06)GOTO190
  IT = IT + 1
  IF(IT.GT.10)GOTO190
  IF(PA.LT.P)GOTO160
  
```

```

160 EL = E
    GOT0150
170 ER = E
    GOT0150
165 IF(P.GT.PSI(NODE(I,3)))GOTO180
    EL = E1(3)
    ER = E1(4)
    GOT0150
C     CHECK NEXT ELEMENT ABOVE PRESENT ELEMENT
180 IF(KK.GT.0)GOTO185
    IF(I.EQ.1)GOTO165
    I = I - 1
    GOT0140
185 IF(I.EQ.1.AND.N.EQ.2)GOTO187
    IF(I.EQ.1.AND.N.EQ.8)GOTO187
    I = I - 1
    GOT0140
    I = I
    GOT0165
C     CONVERGENCE CRITERIA SATISFIED.
C     CHECK TO SEE WHAT TYPE OF ELEMENT.
190 IF(NTE(II).EQ.3)GOTO195
    IF(NTE(II).EQ.2)GOTO196
        CALCULATE WHIRL AND STATIC ENTHALPY(DUCT)
        WRL(NODE(II,N)) = SF(3)*WRL(NODE(I,3)) + SF(4)*WRL(NODE(I,4))
        I + SF(5)*WRL(NODE(I,5))
        HS(NODE(II,N)) = SF(3)*HS(NODE(I,3)) + SF(4)*HS(NODE(I,4))
        I + SF(5)*HS(NODE(I,5))
        TVEL(NODE(II,N)) = WRL(NODE(II,N))/RC(NODE(II,N))
C     CALCULATE TOT ENTHALPY AT THE NODE.
C     H(NODE(II,N)) = UVEL(NODE(II,N))*2*(1.DO + DTAN(ALP(NODE(II,N))))*
        I*2)
        H(NODE(II,N)) = H(NODE(II,N)) + VVEL(NODE(II,N))*2
        H(NODE(II,N)) = HS(NODE(II,N)) + H(NODE(II,N))/7.20935D06
        GOT0199
C     CALCULATE TOT ENTHALPY AT NODE(STATOR).
C     H(NODE(II,N)) = SF(3)*H(NODE(I,3)) + SF(4)*H(NODE(I,4)) + SF(5)*
        I H(NODE(I,5))
C     CALCULATE TVEL,SWHIRL,AND STATIC ENTHALPY AT NODE(STATOR)
C     VZ = UVEL(NODE(II,N))
STR10080
STR10090
STR10100
STR10110
STR10120
STR10130
STR10140
STR10150
STR10160
STR10170
STR10180
STR10190
STR10200
STR10210
STR10220
STR10230
STR10240
STR10250
STR10260
STR10270
STR10280
STR10290
STR10300
STR10310
STR10320
STR10330
STR10340
STR10350
STR10360
STR10370
STR10380
STR10390
STR10400
STR10410
STR10420
STR10430
STR10440
STR10450
STR10460
STR10470
STR10480
STR10490
STR10500
STR10510
STR10520
STR10530
STR10540
STR10550

```



STR11040  
 STR11050  
 STR11060  
 STR11070  
 MPL00010  
  
 MPL00040  
 MPL00060  
  
 MPL00090  
 MPL00100  
 MPL00110  
 MPL00130  
 MPL00140  
 MPL00150  
  
 MPL00180  
  
 MPL00220  
  
 MPL00260  
 MPL00270  
 MPL00280  
 MPL00290  
 MPL00340  
 MPL00350  
 MPL00360

```

SF(8) = (1.D0 - E*E + Z - Z*E*E)/2.D0
RETURN
DEBUG SUBCHK
END
SUBROUTINE MPLOTRC(ZC, ZC, NODE, NN, NE)
  IMPLICIT REAL*8(A-H, P-Z)
  DIMENSION RC(NN), ZC(NN), OP1(9), OP2(9)
  DIMENSION O1(107), O2(107)
  DIMENSION NODE(NE, 8)
  REAL*8 TITLE(3), GAVITO, 'NASA', 'TASK 1'
  DATA OSCALE / .24 /
  DO 100 L = 1, NN
    O1(L) = ZC(L)*OSCALE
    O2(L) = RC(L)*OSCALE
  CONTINUE
  CALL PLOTS
  CALL PLOT(0, 0, 3, 0, -3)
  DO 200 I = 1, NE
    NPE = 9
    DO 300 J = 1, 8
      OP1(J) = O1(NODE(I, J))
      OP2(J) = O2(NODE(I, J))
    CONTINUE
    CP1(NPE) = OP1(1)
    CP2(NPE) = OP2(1)
    CALL LINE(OP1, OP2, NPE, 1, 1)
  CONTINUE
  DO 400 K = 1, NN
    OL = FLOAT(K)
    CALL NUMBER(O1(K), O2(K), .07, OL, 0, -1)
  CONTINUE
  CALL SYMBOL(0, 0, 5, 0, 14, TITLE, 0, 0, 24)
  CALL PLOT(0, 0, 7, 0, -3)
  CALL PLOTE
  RETURN
DEBUG SUBCHK
END
  
```

100

300

200

400

APPENDIX B  
 SAMPLE INPUT DATA

NASA TASK-1 IC7	TRANSONIC COMPRESSOR	COMPRESSOR	
1	0.00	18.878	1.
2	.00	17.439	1.
3	.00	16.0	1.
4	.00	14.5	1.
5	.00	13.0	1.
6	.00	11.5	1.
7	.00	10.0	1.
8	.00	8.5495	1.
9	0.	7.099	1.
10	3.	18.484	1.
11	3.	16.0	1.
12	3.	13.0	1.
13	3.	10.0	1.
14	3.	7.099	1.
15	6.	18.409	1.
16	6.	17.205	1.
17	6.	16.0	1.
18	6.	14.5	1.
19	6.	13.0	1.
20	6.	11.5	1.
21	6.	10.0	1.
22	6.	8.5495	1.
23	6.	7.099	1.
24	8.902	18.403	1.
25	8.902	15.798	1.
26	8.902	12.897	1.
27	8.902	9.996	1.
28	8.902	7.145	1.
29	11.804	18.397	1.
30	11.804	16.996	1.
31	11.804	15.595	1.
32	11.804	14.194	1.
33	11.804	12.793	1.
34	11.804	11.392	1.
35	11.804	9.991	1.
36	11.804	8.591	1.
37	15.5	7.19	1.
38	15.5	18.37	1.
39	15.5	15.835	1.
40	15.5	13.3	1.
41	15.5	10.765	1.
42	15.5	8.23	1.
43	18.511	18.25	1.
44	18.447	17.161	1.
45	18.383	16.072	1.
46	18.319	14.855	1.
			.9921628
			.991016
			.989867
			.988101

47	18.256	13.638	.986334
48	18.192	12.659	.984340
49	18.128	11.68	.982346
50	18.064	10.403	.978950
51	18.522	9.125	.975533
52	19.524	18.037	.931421
53	19.527	16.037	.896215
54	19.528	13.778	.858371
55	19.53	11.634	.792201
56	20.533	9.871	.991146
57	20.599	17.937	.989867
58	20.665	16.002	.988100
59	20.731	14.888	.986336
60	20.797	13.773	.984242
61	20.862	12.824	.982148
62	20.928	11.875	.989852
63	20.994	11.009	.997555
64	21.06	10.142	1.
65	21.692	17.838	1.
66	21.802	15.822	1.
67	21.911	14.86	1.
68	22.031	12.286	1.
69	22.13	10.348	.988014
70	22.85	17.836	.987362
71	22.904	17.711	.987650
72	22.958	16.586	.986970
73	22.962	15.589	.986091
74	23.028	14.859	.985934
75	23.062	14.132	.984777
76	23.096	13.415	.983765
77	23.148	12.698	.982754
78	23.2	11.625	.902895
79	23.225	10.553	.904725
80	24.615	17.836	.903892
81	24.610	15.642	.902994
82	24.610	14.228	.988014
83	24.605	12.852	.987362
84	24.6	10.831	.987650
85	24.4	17.836	.986970
86	26.336	16.767	.986091
87	26.273	15.697	.98543
88	26.232	15.011	.98477
89	26.191	14.325	.983762
90	26.152	13.665	1.
91	26.113	13.005	
92	26.056	12.057	
93	26.0	11.109	
94	29.7	17.839	



755553  
•755379  
•755029  
•721694  
•688183  
•63146  
•574737  
•475777  
•376817  
•723788  
•703717  
•710175  
•670003  
•624479  
•692198  
•672301  
•652404  
•692372  
•732166  
•748921  
•765501  
•871094  
•871966  
•692198  
•652404  
•732166  
•75721

111112222111133331111  
43  
44  
45  
46  
47  
48  
49  
50  
51  
52  
53  
54  
55  
56  
57  
58  
59  
60  
61  
62  
63  
64  
65  
66  
67  
68  
69

89  
10  
11  
12  
13  
14  
15  
16  
17  
18  
19  
20  
21  
22  
23  
24  
25  
26  
27  
28

70	.871967
71	.692198
72	.672301
73	.652404
74	.692372
75	.732166
76	.740544
77	.748921
78	.810444
79	.871967
80	.346099
81	.326202
82	.36617
83	.40300
84	.435983

STOP

43	1.08
44	1.0369
45	.993791
46	.950681
47	.907571
48	.881915
49	.856259
50	.823534
51	.790809
52	1.040565
53	.967785
54	.831475
55	.707731
56	.477173
57	1.001121
58	.97145
59	.941605
60	.848405
61	.755204
62	.657117
63	.559029
64	.361283
65	.163537

107.6	STOP	201.482573318.846572	.08192	.08	15.0546	499.38
4359.5						
53.35						
17.1250719		1.4				

.240

1017.1250719
1517.1250719
2417.1250719
2917.1250719



46  
47  
48  
49  
50  
53  
54  
55  
58  
59  
60  
61  
62  
63  
64  
67  
68  
69  
72  
73  
74  
75  
76  
77  
78  
81  
82  
83  
86  
87  
88  
89  
90  
91  
92  
95  
96  
97

STOP

APPENDIX C  
 SAMPLE OUTPUT LISTING

NASA TASK-1 TRANSONIC COMPRESSOR  
 NO. OF NODES = 107

NODE	NO. OF ELEMENTS	Z (I)	SUMMARY OF NODAL COORDINATES	REL FLOW ANG	ABS FLOW ANG
1	0	0.0	R (I)	0.0	0.0
2	0	0.0	0.188780D 02	0.0	0.0
3	0	0.0	0.174390D 02	0.0	0.0
4	0	0.0	0.160000D 02	0.0	0.0
5	0	0.0	0.145000D 02	0.0	0.0
6	0	0.0	0.130000D 02	0.0	0.0
7	0	0.0	0.115000D 02	0.0	0.0
8	0	0.0	0.100000D 02	0.0	0.0
9	0	0.0	0.854950D 01	0.0	0.0
10	0	0.0	0.709900D 01	0.0	0.0
11	0	0.300000D 01	0.184840D 02	0.0	0.0
12	0	0.300000D 01	0.160000D 02	0.0	0.0
13	0	0.300000D 01	0.130000D 02	0.0	0.0
14	0	0.300000D 01	0.100000D 02	0.0	0.0
15	0	0.600000D 01	0.709900D 01	0.0	0.0
16	0	0.600000D 01	0.184090D 02	0.0	0.0
17	0	0.600000D 01	0.172050D 02	0.0	0.0
18	0	0.600000D 01	0.160000D 02	0.0	0.0
19	0	0.600000D 01	0.145000D 02	0.0	0.0
20	0	0.600000D 01	0.130000D 02	0.0	0.0
21	0	0.600000D 01	0.115000D 02	0.0	0.0
22	0	0.600000D 01	0.100000D 02	0.0	0.0
23	0	0.600000D 01	0.854950D 01	0.0	0.0
24	0	0.890200D 01	0.709900D 01	0.0	0.0
25	0	0.890200D 01	0.184030D 02	0.0	0.0
26	0	0.890200D 01	0.157980D 02	0.0	0.0
27	0	0.890200D 01	0.128970D 02	0.0	0.0
28	0	0.890200D 01	0.999600D 01	0.0	0.0
29	0	0.118040D 02	0.714500D 01	0.0	0.0
30	0	0.118040D 02	0.183970D 02	0.0	0.0
31	0	0.118040D 02	0.169960D 02	0.0	0.0
32	0	0.118040D 02	0.155950D 02	0.0	0.0
33	0	0.118040D 02	0.141940D 02	0.0	0.0
34	0	0.118040D 02	0.127940D 02	0.0	0.0
35	0	0.118040D 02	0.113930D 02	0.0	0.0
36	0	0.118040D 02	0.999200D 01	0.0	0.0
37	0	0.155000D 02	0.859100D 01	0.0	0.0
38	0	0.155000D 02	0.719000D 01	0.0	0.0
39	0	0.155000D 02	0.183700D 02	0.0	0.0
40	0	0.155000D 02	0.158350D 02	0.0	0.0
41	0	0.155000D 02	0.133000D 02	0.0	0.0
42	0	0.155000D 02	0.107650D 02	0.0	0.0
			0.823000D 01	0.0	0.0

43	0.	1851	100	02	0.	1825	000	00	0.	9921	630	00	0.	7555	530	00	0.	1080	000	01	0.	1036	900	01
44	0.	1844	700	02	0.	1716	100	00	0.	9910	160	00	0.	7553	790	00	0.	9933	791	00	0.	9506	810	00
45	0.	1838	300	02	0.	1607	200	00	0.	9898	670	00	0.	7550	290	00	0.	9507	910	00	0.	9075	710	00
46	0.	1831	900	02	0.	1485	500	00	0.	9881	010	00	0.	7216	940	00	0.	9075	710	00	0.	8819	150	00
47	0.	1825	600	02	0.	1363	800	00	0.	9863	340	00	0.	6881	830	00	0.	8819	150	00	0.	8562	590	00
48	0.	1819	200	02	0.	1265	900	00	0.	9843	340	00	0.	6314	600	00	0.	8562	590	00	0.	8233	530	00
49	0.	1812	800	02	0.	1168	000	00	0.	9823	340	00	0.	5747	370	00	0.	7908	090	00	0.	1040	570	01
50	0.	1806	400	02	0.	1104	030	00	0.	9789	500	00	0.	4757	770	00	0.	1040	570	01	0.	9677	850	00
51	0.	1800	000	02	0.	9125	000	00	0.	9755	530	00	0.	3768	170	00	0.	9677	850	00	0.	8314	750	00
52	0.	1952	200	02	0.	1801	000	00	0.	9542	280	00	0.	7223	780	00	0.	8314	750	00	0.	7077	310	00
53	0.	1952	400	02	0.	1603	700	00	0.	9314	210	00	0.	7037	170	00	0.	7077	310	00	0.	4771	730	00
54	0.	1952	700	02	0.	1370	600	00	0.	8962	150	00	0.	7101	150	00	0.	4771	730	00	0.	1001	120	01
55	0.	1952	800	02	0.	1177	800	00	0.	8583	710	00	0.	6700	030	00	0.	9714	500	00	0.	9416	050	00
56	0.	1953	000	02	0.	9633	400	00	0.	7922	200	00	0.	6244	790	00	0.	9416	050	00	0.	8484	050	00
57	0.	2053	300	02	0.	1787	100	00	0.	9924	240	00	0.	6921	980	00	0.	7552	040	00	0.	5590	290	00
58	0.	2059	900	02	0.	1693	700	00	0.	9911	450	00	0.	6723	010	00	0.	5590	290	00	0.	3612	830	00
59	0.	2066	500	02	0.	1600	200	00	0.	9898	670	00	0.	6522	400	00	0.	3612	830	00	0.	1635	370	00
60	0.	2073	100	02	0.	1488	800	00	0.	9881	000	00	0.	6921	980	00	0.	1635	370	00	0.	0.	0.	0.
61	0.	2079	700	02	0.	1377	300	00	0.	9863	360	00	0.	6522	400	00	0.	0.	0.	0.	0.	0.	0.	0.
62	0.	2086	200	02	0.	1282	400	00	0.	9842	420	00	0.	7321	660	00	0.	0.	0.	0.	0.	0.	0.	0.
63	0.	2092	800	02	0.	1187	500	00	0.	9821	480	00	0.	7489	210	00	0.	0.	0.	0.	0.	0.	0.	0.
64	0.	2099	400	02	0.	1100	900	00	0.	9898	520	00	0.	7655	010	00	0.	0.	0.	0.	0.	0.	0.	0.
65	0.	2106	000	02	0.	1014	200	00	0.	9975	550	00	0.	8710	940	00	0.	0.	0.	0.	0.	0.	0.	0.
66	0.	2169	200	02	0.	1783	800	00	0.	1000	000	01	0.	8719	660	00	0.	0.	0.	0.	0.	0.	0.	0.
67	0.	2180	200	02	0.	1582	200	00	0.	1000	000	01	0.	6921	980	00	0.	0.	0.	0.	0.	0.	0.	0.
68	0.	2191	100	02	0.	1400	000	00	0.	1000	000	01	0.	7321	660	00	0.	0.	0.	0.	0.	0.	0.	0.
69	0.	2203	100	02	0.	1228	600	00	0.	1000	000	01	0.	7572	100	00	0.	0.	0.	0.	0.	0.	0.	0.
70	0.	2213	000	02	0.	1034	800	00	0.	1000	000	01	0.	8719	670	00	0.	0.	0.	0.	0.	0.	0.	0.
71	0.	2285	000	02	0.	1783	600	00	0.	9880	140	00	0.	6921	980	00	0.	0.	0.	0.	0.	0.	0.	0.
72	0.	2290	400	02	0.	1671	100	00	0.	9873	620	00	0.	6522	400	00	0.	0.	0.	0.	0.	0.	0.	0.
73	0.	2295	800	02	0.	1558	600	00	0.	9869	700	00	0.	6522	400	00	0.	0.	0.	0.	0.	0.	0.	0.
74	0.	2296	200	02	0.	1485	900	00	0.	9860	910	00	0.	7321	660	00	0.	0.	0.	0.	0.	0.	0.	0.
75	0.	2302	800	02	0.	1413	200	00	0.	9860	910	00	0.	7321	660	00	0.	0.	0.	0.	0.	0.	0.	0.
76	0.	2306	200	02	0.	1341	500	00	0.	9859	340	00	0.	7405	440	00	0.	0.	0.	0.	0.	0.	0.	0.
77	0.	2309	600	02	0.	1269	800	00	0.	9847	770	00	0.	7489	210	00	0.	0.	0.	0.	0.	0.	0.	0.
78	0.	2314	800	02	0.	1162	500	00	0.	9837	650	00	0.	8104	440	00	0.	0.	0.	0.	0.	0.	0.	0.
79	0.	2320	000	02	0.	1055	300	00	0.	9827	540	00	0.	8719	670	00	0.	0.	0.	0.	0.	0.	0.	0.
80	0.	2462	500	02	0.	1783	600	00	0.	9026	110	00	0.	3460	990	00	0.	0.	0.	0.	0.	0.	0.	0.
81	0.	2461	500	02	0.	1564	200	00	0.	9028	950	00	0.	3262	020	00	0.	0.	0.	0.	0.	0.	0.	0.
82	0.	2461	000	02	0.	1422	800	00	0.	9047	250	00	0.	3661	700	00	0.	0.	0.	0.	0.	0.	0.	0.
83	0.	2460	500	02	0.	1285	200	00	0.	9038	920	00	0.	4030	000	00	0.	0.	0.	0.	0.	0.	0.	0.
84	0.	2460	000	02	0.	1083	100	00	0.	9029	940	00	0.	0.	0.	0.	0.	0.	0.	0.	0.	0.	0.	0.
85	0.	2640	000	02	0.	1783	600	00	0.	9880	140	00	0.	0.	0.	0.	0.	0.	0.	0.	0.	0.	0.	0.
86	0.	2627	300	02	0.	1676	700	00	0.	9873	620	00	0.	0.	0.	0.	0.	0.	0.	0.	0.	0.	0.	0.
87	0.	2623	200	02	0.	1569	700	00	0.	9876	500	00	0.	0.	0.	0.	0.	0.	0.	0.	0.	0.	0.	0.
88	0.	2623	200	02	0.	1501	100	00	0.	9869	700	00	0.	0.	0.	0.	0.	0.	0.	0.	0.	0.	0.	0.
89	0.	2619	100	02	0.	1432	500	00	0.	9860	910	00	0.	0.	0.	0.	0.	0.	0.	0.	0.	0.	0.	0.
90	0.	2615	200	02	0.	1366	500	00	0.	9854	300	00	0.	0.	0.	0.	0.	0.	0.	0.	0.	0.	0.	0.

91	0.	2611300	02	0.	1300500	02	0.	9847700	00	0.	0.
92	C.	2605600	02	0.	1205700	02	0.	9837620	00	0.	0.
93	0.	2600000	02	0.	1110900	02	0.	9827540	00	0.	0.
94	0.	2970000	02	0.	1783900	02	0.	1000000	01	0.	0.
95	0.	2965000	02	0.	1594900	02	0.	1000000	01	0.	0.
96	0.	2960000	02	0.	1441300	02	0.	1000000	01	0.	0.
97	0.	2955000	02	0.	1290000	02	0.	1000000	01	0.	0.
98	0.	2950000	02	0.	1114000	02	0.	1000000	01	0.	0.
99	0.	3300000	02	0.	1783600	02	0.	1000000	01	0.	0.
100	0.	3300000	02	0.	1701800	02	0.	1000000	01	0.	0.
101	C.	3300000	02	0.	1620000	02	0.	1000000	01	0.	0.
102	0.	3300000	02	0.	1535000	02	0.	1000000	01	0.	0.
103	0.	3300000	02	0.	1450000	02	0.	1000000	01	0.	0.
104	0.	3300000	02	0.	1365000	02	0.	1000000	01	0.	0.
105	C.	3300000	02	0.	1280000	02	0.	1000000	01	0.	0.
106	0.	3300000	02	0.	1198500	02	0.	1000000	01	0.	0.
107	0.	3300000	02	0.	1117000	02	0.	1000000	01	0.	0.

SYSTEM TOPOLOGY

NODES

ELEMENT

TYPE OF ELEMENT

15	1	17	19	29	33	35	43	47	49	57	59	61	63	71	73	75	77	85	87	89	99	101	103	105				
1	2	3	4	5	6	7	8	9	10	11	12	13	14	15	16	17	18	19	20	21	22	23	24	25	26	27	28	
1	1	1	1	1	1	1	1	1	1	1	1	1	1	1	1	1	1	1	1	1	1	1	1	1	1	1		
16	18	20	22	30	32	34	36	44	46	48	50	58	60	62	64	72	74	76	78	86	88	90	92	100	102	104	106	
17	19	21	23	31	33	35	37	45	47	49	51	59	61	63	65	73	75	77	79	87	89	91	93	101	103	105	107	
3	5	7	9	17	19	21	23	31	33	35	37	45	47	49	51	59	61	63	65	73	75	77	79	87	89	91	93	
11	12	13	14	25	26	27	28	39	40	41	42	43	45	46	55	56	57	68	69	70	81	82	83	84	85	96	97	98
1	1	1	1	1	1	1	1	1	1	1	1	1	1	1	1	1	1	1	1	1	1	1	1	1	1	1	1	

INLET THERMODYNAMIC VARIABLES ARE AS FOLLOWS

FLOW RATE = 0.107600D 03 LBM/SEC  
 TOT DENSITY = 0.819200D-01 LBM CU FT  
 TOT PRESSURE = 0.150546 D 02 PSI  
 TOT TEMPERATURE = 0.499380D 03 DEG RANKINE  
 ROTATIONAL SPEED = 0.435950D 04 RPM  
 INLET U VELOCITY = 0.201483D 03 FT/SEC  
 OUTLET U VELOCITY = 0.318847D 03 FT/SEC  
 GAS CONSTANT = 0.533500D 02  
 RATIO OF SPECIFIC HEATS = 0.140000D 01  
 SPECIFIC HEAT AT CONSTANT PRESSURE = 0.240000D 00  
 STATIC DENSITY AT INLET = 0.800000D-01  
 INITIAL ESTIMATE OF PSI DISTRIBUTION = 0.171251D 02  
 NODES WHERE PSI IS SPECIFIED

NODE NO.	PSI (I)
10	0.171251D 02
15	0.171251D 02
24	0.171251D 02
29	0.171251D 02
38	0.171251D 02
43	0.171251D 02
52	0.171251D 02
57	0.171251D 02
66	0.171251D 02
71	0.171251D 02
80	0.171251D 02
85	0.171251D 02
94	0.171251D 02
14	0.0
23	0.0
28	0.0
37	0.0
42	0.0
51	0.0
56	0.0

```

65 0.0
70 0.0
84 0.0
93 0.0
98 0.0
1 0.171251D 02
2 0.142002D 02
3 0.115071D 02
4 0.894662D 01
5 0.663797D 01
6 0.458117D 01
7 0.277622D 01
8 0.127036D 01
9 0.0
99 0.171251D 02
100 0.145999D 02
101 0.121933D 02
102 0.981814D 01
103 0.757093D 01
104 0.545171D 01
105 0.346047D 01
106 0.167140D 01
107 0.0

```

NODES WHERE F(R,Z) IS SPECIFIED

```

NODE NO. 13 16 17 18 19 20 21
          25 27 30 31 32 33 34
          36 40 41 44 45 46 47
          49 53 54 55 58 59 60
          62 64 67 68 69 72 73
          75 77 78 81 82 83 86
          88 89 90 91 92 95 96 97

```

LARGEST EPS FOR ITERATION 1 IS 0.136047897529D 02  
ITERATION NO. 1 COMPLETE  
STREAM FUNCTION CONVERGENCE NOT YET SATISFIED.  
NEXT ITERATION IS IN PROGRESS  
LARGEST EPS FOR ITERATION 2 IS 0.442913378700D 00  
PROGRAM TERMINATED ON ITERATION NO. 2  
RESULTS WHICH FOLLOW ARE FOR CONVERGENCE EPSILON = 0.442913378700D 00

FINITE ELEMENT RESULTS

NODE	PSI (I)	VZ	VR	R (I)	DENSITY
1	0.1712510	0.2014830	0.0	0.1887800	0.8000000-01
2	0.1420020	0.2014830	0.0	0.1743900	0.8000000-01
3	0.1150710	0.2014830	0.0	0.1600000	0.8000000-01
4	0.8946620	0.2014830	0.0	0.1450000	0.8000000-01
5	0.6637970	0.2014830	0.0	0.1300000	0.8000000-01
6	0.4581170	0.2014830	0.0	0.1150000	0.8000000-01
7	0.2776220	0.2014830	0.0	0.1000000	0.8000000-01
8	0.1270360	0.2014830	0.0	0.8549500	0.8000000-01
9	0.0	0.2014830	0.0	0.7099000	0.8000000-01
10	0.1712510	0.2200590	-0.1720130	0.1848400	0.8027340-01
11	0.1184450	0.2100360	-0.140730	0.1600000	0.8042970-01
12	0.6782560	0.2061220	-0.7301550	0.1300000	0.8046870-01
13	0.2825030	0.2026210	-0.2723300	0.1000000	0.8050780-01
14	0.0	0.2053470	0.0	0.7099000	0.8048830-01
15	0.1712510	0.2119020	-0.4381160	0.1840900	0.8039060-01
16	0.1456300	0.2165730	-0.4651150	0.1720500	0.8031250-01
17	0.1211880	0.2165450	-0.1587810	0.1600000	0.8031250-01
18	0.9378870	0.2125850	-0.6798830	0.1450000	0.8039060-01
19	0.6956220	0.2138670	-0.6842640	0.1300000	0.8035160-01
20	0.4770520	0.2122840	-0.6730670	0.1150000	0.8039060-01
21	0.2867570	0.2046430	-0.5647210	0.1000000	0.8050780-01
22	0.1320900	0.2069000	-0.2252770	0.8549500	0.8046870-01
23	0.0	0.2100410	0.0	0.7099000	0.8042970-01
24	0.1712510	0.2276750	-0.4707280	0.1840300	0.8015620-01
25	0.1197350	0.2056880	-0.1660290	0.1579800	0.8046870-01
26	0.7021330	0.2202630	-0.1481560	0.1289700	0.8025390-01
27	0.2926640	0.2263960	-0.2236320	0.9996000	0.8019530-01
28	0.0	0.1983060	0.0	0.7145000	0.8056640-01
29	0.1712510	0.2264290	-0.3109210	0.1839700	0.8017580-01
30	0.1427760	0.1836100	-0.7956510	0.1699600	0.8054690-01
31	0.1223410	0.2065300	-0.1664550	0.1559500	0.7953120-01
32	0.9741050	0.2281870	-0.1727250	0.1419400	0.7914060-01
33	0.7248150	0.2418880	-0.1796600	0.1279400	0.7886720-01
34	0.4981240	0.2456540	-0.1308260	0.1139300	0.7929690-01
35	0.2929740	0.2458730	-0.6625080	0.9992000	0.7972660-01
36	0.1244480	0.2182740	-0.1833150	0.8591000	0.8029300-01
37	0.0	0.1813160	0.0	0.7190000	0.8074220-01
38	0.1712510	0.9537140	-0.2090290	0.1837000	0.8160160-01
39	0.1561180	0.2112830	-0.4885000	0.1583500	0.8039060-01
40	0.1074470	0.3413290	0.1244780	0.1330000	0.7800780-01
41	0.4676010	0.3591520	0.4199680	0.1076500	0.7753910-01
42	0.0	0.3651270	0.1140290	0.8230000	0.7703120-01
43	0.1712510	0.1889150	-0.5428270	0.1825000	0.8367190-01
44	0.1502360	0.1829830	-0.3637860	0.1716100	0.8406250-01
45	0.1312220	0.1813770	-0.3580190	0.1607200	0.8351560-01

46	0.109989D 02	0.217508D 03	-0.332291D 02	0.148550D 02	0.804687D-01
47	0.874510D 01	0.263002D 03	-0.321793D 02	0.136380D 02	0.771484D-01
48	0.684972D 01	0.300928D 03	-0.128776D 02	0.126590D 02	0.751172D-01
49	0.490441D 01	0.357638D 03	0.801256D 01	0.116800D 02	0.718555D-01
50	0.237289D 01	0.385140D 03	0.629724D 02	0.104030D 02	0.710547D-01
51	0.0	0.433195D 03	0.144257D 03	0.912500D 01	0.681250D-01
52	0.171251D 02	0.242434D 03	-0.454414D 02	0.180100D 02	0.800000D-01
53	0.132234D 02	0.208945D 03	0.543975D 01	0.160370D 02	0.826172D-01
54	0.883947D 01	0.334585D 03	0.477602D 02	0.137060D 02	0.726172D-01
55	0.476760D 01	0.538251D 03	0.107145D 03	0.117780D 02	0.600391D-01
56	0.0	0.684311D 03	0.227433D 03	0.963400D 01	0.600391D-01
57	0.171251D 02	0.281327D 03	-0.117674D 02	0.178710D 02	0.800000D-01
58	0.147764D 02	0.236773D 03	0.134070D 02	0.169370D 02	0.817578D-01
59	0.128904D 02	0.217194D 03	0.529913D 02	0.160020D 02	0.825391D-01
60	0.106224D 02	0.252037D 03	0.812332D 02	0.148880D 02	0.789453D-01
61	0.827315D 01	0.303197D 03	0.114025D 03	0.137730D 02	0.743359D-01
62	0.619073D 01	0.341721D 03	0.132514D 03	0.128240D 02	0.717969D-01
63	0.408225D 01	0.401864D 03	0.150547D 03	0.118750D 02	0.681836D-01
64	0.207387D 01	0.491840D 03	0.147459D 03	0.110090D 02	0.618750D-01
65	0.0	0.567354D 03	-0.109494D 03	0.101420D 02	0.600391D-01
66	0.171251D 02	0.302506D 03	0.456957D 01	0.178380D 02	0.767383D-01
67	0.120681D 02	0.255341D 03	0.349385D 02	0.158220D 02	0.783984D-01
68	0.798850D 01	0.300666D 03	0.802308D 02	0.140000D 02	0.762500D-01
69	0.417127D 01	0.334517D 03	0.980101D 02	0.128260D 02	0.745703D-01
70	0.0	0.445955D 03	0.856484D 02	0.103480D 02	0.662695D-01
71	0.171251D 02	0.301848D 03	0.307300D-12	0.178360D 02	0.767578D-01
72	0.140702D 02	0.292879D 03	0.105376D 02	0.167110D 02	0.772070D-01
73	0.112853D 02	0.299853D 03	0.288777D 02	0.155860D 02	0.771094D-01
74	0.950536D 01	0.310703D 03	0.432738D 02	0.148590D 02	0.764062D-01
75	0.774640D 01	0.328817D 03	0.559861D 02	0.141320D 02	0.753125D-01
76	0.606420D 01	0.326266D 03	0.632255D 02	0.134150D 02	0.752734D-01
77	0.448194D 01	0.328199D 03	0.724202D 02	0.126980D 02	0.750781D-01
78	0.220067D 01	0.357466D 03	0.758258D 02	0.116250D 02	0.728516D-01
79	0.0	0.401487D 03	0.797238D 02	0.105530D 02	0.690625D-01
80	0.171251D 02	0.338282D 03	0.0	0.178360D 02	0.775781D-01
81	0.110657D 02	0.357678D 03	0.267016D 02	0.156420D 02	0.771094D-01
82	0.742061D 01	0.358663D 03	0.434724D 02	0.142280D 02	0.769141D-01
83	0.420615D 01	0.347499D 03	0.534363D 02	0.128520D 02	0.770312D-01
84	0.0	0.390797D 03	0.776011D 02	0.108310D 02	0.755273D-01
85	0.171251D 02	0.312169D 03	0.567579D 00	0.178360D 02	0.786328D-01
86	0.139682D 02	0.316128D 03	-0.126945D 03	0.167670D 02	0.780078D-01
87	0.109162D 02	0.335360D 03	0.277874D 03	0.156970D 02	0.755859D-01
88	0.902395D 01	0.324992D 03	-0.331898D 03	0.150110D 02	0.747656D-01
89	0.727694D 01	0.322973D 03	-0.392978D 03	0.143250D 02	0.733594D-01
90	0.567134D 01	0.320579D 03	-0.356204D 03	0.136650D 02	0.743164D-01
91	0.414305D 01	0.319875D 03	-0.318186D 03	0.130050D 02	0.751562D-01
92	0.203268D 01	0.333436D 03	-0.163312D 03	0.120570D 02	0.773047D-01
93	0.0	0.357598D 03	0.321838D 01	0.111090D 02	0.776172D-01





82	0	244303D	05	0	124673D	03	0	143088D	03	0	0
83	0	265507D	05	0	127365D	03	0	172157D	03	0	0
84	0	326492D	05	0	134132D	03	0	251202D	03	0	0
85	0	0	0	0	119987D	03	0	0	0	0	0
86	0	0	0	0	120783D	03	0	0	0	0	0
87	0	0	0	0	122067D	03	0	0	0	0	0
88	0	0	0	0	123223D	03	0	0	0	0	0
89	0	0	0	0	124821D	03	0	0	0	0	0
90	0	0	0	0	126075D	03	0	0	0	0	0
91	0	0	0	0	127436D	03	0	0	0	0	0
92	0	0	0	0	130339D	03	0	0	0	0	0
93	0	0	0	0	134132D	03	0	0	0	0	0
94	0	0	0	0	120279D	03	0	0	0	0	0
95	0	0	0	0	122120D	03	0	0	0	0	0
96	0	0	0	0	125018D	03	0	0	0	0	0
97	0	0	0	0	127731D	03	0	0	0	0	0
98	0	0	0	0	132648D	03	0	0	0	0	0
99	0	0	0	0	120854D	03	0	0	0	0	0
100	0	0	0	0	121376D	03	0	0	0	0	0
101	0	0	0	0	122195D	03	0	0	0	0	0
102	0	0	0	0	123484D	03	0	0	0	0	0
103	0	0	0	0	125192D	03	0	0	0	0	0
104	0	0	0	0	126543D	03	0	0	0	0	0
105	0	0	0	0	128131D	03	0	0	0	0	0
106	0	0	0	0	129812D	03	0	0	0	0	0
107	0	0	0	0	131572D	03	0	0	0	0	0

## APPENDIX D

### CALCULATION OF ROTOR ELEMENT FLOW ANGLES

The following is a brief synopsis of the procedure contained in Ref.13 for calculating the outlet relative flow angles in a rotor element from the given inlet relative flow angle and blade solidity. The reader is referred to Ref.13, Chapter VI, for specific details of low speed correlation data.

As stated in Section III.A, uniform flow conditions at the rotor blade edges were assumed. This assumption coupled with knowledge of the mass flow rate and rotational speed, enables one to calculate the inlet relative flow angle,  $\beta_1$ , as shown in Fig 18.

From blade geometry information, the blade solidity,  $\sigma$ ,

$$\sigma = \frac{c}{s} \quad (1)$$

is obtained. At this point,  $\beta_1$ , and  $\sigma$  are given and one may calculate  $\beta_2$ , the rotor outlet relative flow angle from correlation curves depicted in Ref 13. The equation used to determine  $\beta_2$ , is the following,

$$\beta_2 = K_2 + \delta \quad (2)$$

where  $K_2$  is the angle between the tangent to the blade mean

camber line and the axial direction (Fig 18). This is obtained from the blade geometry data.  $\delta$  is the low speed deviation angle which is obtained from the correlation curves in Ref. 13. The following equations show the relationship between  $\delta$  and the correlation data.

$$\delta = \delta_0^\circ + m\phi \quad (3)$$

$$\delta_0^\circ = (KS)_{sh} (KS)_t (\delta_0)_{10} \quad (4)$$

The variables  $m, (KS)_{sh}, (KS)_t$  and  $(\delta_0)_{10}$ , are all values which are obtained from the correlation curves and are all functions of the given blade geometry. The quantity,  $\phi$ , is the blade camber angle and again is obtained from the blade geometry data. Once all the variables are obtained from the correlation data, equation (4) is solved for the deviation angle for an uncambered blade section,  $\delta_0$ , and then equation (3) is solved for the deviation angle,  $\delta$ . One now calculates  $\beta_2$  from equation (2) for the blade element. With  $\beta_2$  now a known quantity, one now calculates the absolute flow angle,  $\alpha_2$ , from uniform flow assumptions.

An example follows for node numbers 43 and 57 (Fig 6). From Ref. [12], Table II, the following quantities are obtained assuming the angle of incidence,  $i$ , (Fig 18) is zero and therefore the inlet relative flow angle,  $\beta_1$ , is equal to  $k_1$ .

$$\beta_1 = k_1 = 61.88^\circ$$

$$\Gamma = 1.3062$$

$$\phi = 6.95^\circ$$

$$K_2 = 54.93^\circ$$

$$\frac{t}{c})_{\max} = 0.035$$

tip radius = 18.25 in

hub radius = 9.125 in

Assuming uniform flow at the rotor inlet and a rotational speed of 4359.5 RPM, the following quantities are determined from the rotor inlet velocity diagram (Fig 18).

$$v_m = \frac{\dot{m}}{\rho A} = \frac{(107.6 \text{ lbm/sec})(144 \text{ in}^2/\text{ft}^2)}{(0.08 \text{ lbm/ft}^3) \pi (18.25^2 - 9.125^2) \text{ in}^2}$$

$$v_m = 246.802 \text{ ft/sec}$$

where the area A, is determined from the hub and tip radii and the density is assumed to be 0.08 lbm/cu ft.

Now one is ready to obtain the correlation data. From Ref.[13], Fig 162, with  $\beta_1 = 61.88^\circ$  and  $\Gamma = 1.3062$ ,

$$\delta_o)_{\omega} = 2.50^\circ$$

From Ref.[13], Fig 162, with  $\beta_1 = 61.88^\circ$  and  $\Gamma = 1.3062$ ,

$$m = 0.235$$

From Ref.[13], Fig 172, with  $t/c)_{\max} = 0.0350$ ,

$$k\delta)t = 0.29$$

From Ref.[13], page 222, one uses the following value of  $(K\delta)_{sh}$  for 65-series blades,

$$(K\delta)_{sh} = 1.0$$

At this point all the necessary data has been obtained for equations (3) and (4),

$$\delta_o^\circ = (1.0)(0.29)(2.50) = 0.725^\circ$$

From equation (3),

$$\delta = 0.725^\circ + 0.235(6.95) = 2.36^\circ$$

Finally, equation (2) gives the desired value of  $\beta_2$ ,

$$\beta_2 = 54.93^\circ + 2.36^\circ = 57.29^\circ$$

At this point the relative flow angle for node 57 has been obtained,  $\beta_2 = 57.29^\circ$ . These two values of relative flow angles,  $\beta_1 = 61.88^\circ$  for node 43 and  $\beta_2 = 57.29^\circ$  for node 57, are then read in the program as input data for numerical computation.

This process is repeated at each required blade element section for the proper outlet relative flow angle.

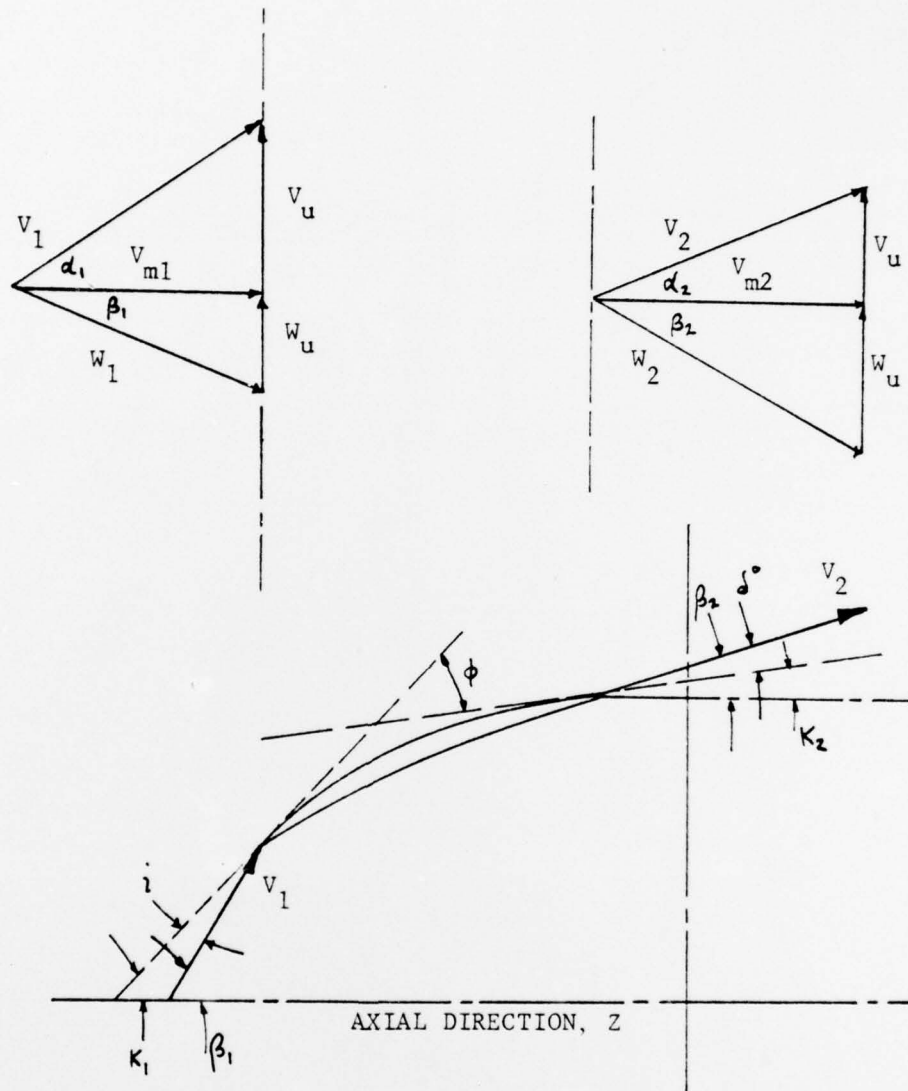


Figure 18 - NOMENCLATURE FOR CASCADE BLADE

LIST OF FIGURES

1. Meridional and Blade-to-Blade Planes.....	9
2. Turbomachine Geometry.....	11
3. Meridional Plane.....	18
4. Isoparametric quadrilateral Element.....	26
5. Gaussian Integration Points.....	31
6. Compressor Discretization.....	33
7. Duct Element.....	35
8. Program Flowchart.....	42
9. Stiffness Matrix Evaluation.....	51
10. SUBROUTINE SLINE.....	57
11. SUBROUTINE FCAL.....	60
12. SUBROUTINE VEL.....	65
13. Axial Profile at Rotor Inlet.....	71
14. Axial Profile at Rotor Outlet.....	72
15. Axial Profile at Stator Inlet.....	73
16. Axial Profile at Stator Outlet.....	74
17. Epsilon vs. Iterations.....	75
18. Nomenclature for Cascade Blade.....	121

## LIST OF REFERENCES

1. NACA TN 2604, A General Theory of Three Dimensional Flow in Subsonic and Supersonic Turbomachines of Axial-, Radial, and Mixed-Flow Type, by C.H. Wu, 1952.
2. Smith, L.H., Jr., 'The Radial Equilibrium Equation of Turbomachinery', ASME Transactions, Journal of Engineering Power, v.88A, p.1-12, 1966.
3. Novak, R.A., 'Streamline Curvature Computing Procedures for Fluid Flow Problems', ASME Transactions, Journal of Engineering Power, v.89A, p.478, 1967.
4. REPORT ME/A-71-5, Carleton University, Division of Aerothermodynamics, A New Computer Program for the Design and Analysis of Turbomachinery, by W.R. Davis, 1971.
5. Wilkinson, D.H., 'Stability, Convergence, and Accuracy of Two-Dimensional Streamline Curvature Methods using Quasi-Orthogonals', Proceedings of the Institute of Mechanical Engineers, v.184, p.108, 1970.
6. Aeronautical Research Council, R and M 3509, A Digital Computer Program for the Through Flow Fluid Mechanics in an Arbitrary Turbomachine using a Matrix Method, by H. Marsh, 1966.
7. Hirsch, CH. and Warzee, G., 'A Finite Element Method for the Axisymmetric Flow Computation in a Turbomachine', International Journal for Numerical Methods in Engineering, v. 10, p.93-113, 1976.
8. Horlock, J.H., 'On Entropy Production in Adiabatic Flow

in Turbomachines', ASME Transactions, Journal of Basic Engineering, v.930, p.587, 1971.

9. Report VUB-STR-5, Vrije Universiteit Brussel, Dept. of Fluid Mechanics, 'A Finite Element Method for Flow Calculations in Turbomachines, by C. Hirsch and G. Warzee, 1974.
10. Huebner, K.H., The Finite Element Method for Engineers, p. 117, Wiley, 1975.
11. Kaplan, W., Advanced Calculus, p. 93, Addison-Wesley, 1952.
12. NASA CR-72806, Vol I., Evaluation of Range and Distortion Tolerance for High Mach Number Transonic Free Stages, by C.C. Koch, K.R. Bilwakesh, and V.L. Doyle, 1971.
13. NASA-SP-36, Aerodynamic Design of Axial Flow Compressors, NASA staff, chap. VI-VII, 1965.
14. Vavra, M.H., Aero-Thermodynamics and Flow in Turbomachines, p. 308, Krieger, 1974.